

STRUCTURALLY DIVERSE HERBICIDES INHIBIT β -KETO-ACYL-CoA SYNTHASES FROM MONOCOTYLEDONOUS AND DICOTYLEDONOUS PLANT SPECIES

Claire Le Ruyet^{a,b}, Stéphanie Pascal^a, Gerlinde Usunow^b, Pierre Van Delft^a, Didier Thoraval^a, François Doignon^a, Frédéric Domergue^a, Peter Luemmen^b and Jérôme Joubès^{a,1}

^a Univ. Bordeaux, CNRS, LBM, UMR 5200, F-33140 Villenave d'Ornon, France

^b Bayer AG, Research & Development, Crop Science, 65926 Frankfurt am Main, Germany

ABSTRACT

Very-long-chain fatty acids (VLCFA) serve as precursors for various lipids that play crucial physiological and structural roles in plants. The β -keto-acyl-CoA synthase (KCS) catalyzes the initial step of VLCFA elongation and determines the chain-length substrate specificity of the fatty acid elongase complex. Following an extensive phylogenetic analysis, 28 KCS genes from various plant species, including 17 functionally uncharacterized genes, were expressed in *Saccharomyces cerevisiae*, and their VLCFAs profiles were analyzed using gas chromatography-mass spectrometry. Yeast expressing active KCS were subsequently exposed *in vivo* to various Group 15 herbicides to investigate their mode of action and selectivity. These experiments revealed differential sensitivities of KCS enzymes to benfuresate, cafenstrole, flufenacet, pyroxasulfone, and metazachlor, while endogenous VLCFA synthesis in yeast, which relies on Elop-type elongases, remained unaffected. Furthermore, to address a significant gap in understanding the inhibitory potency of Group 15 herbicides, we developed an *in vitro* enzymatic assay based on the quantification of the 3-oxo-products generated during the KCS-catalyzed reaction using high-performance liquid chromatography-mass spectrometry coupled with UV detection. This novel biochemical approach enabled the evaluation of inhibitor potency as well as the kinetic characterization of both established and newly identified KCS enzyme inhibitors.

STRUCTURALLY DIVERSE HERBICIDES INHIBIT β -KETO-ACYL-CoA SYNTHASES FROM MONOCOTYLEDONOUS AND DICOTYLEDONOUS PLANT SPECIES

Claire Le Ruyet^{a,b}, Stéphanie Pascal^a, Gerlinde Usunow^b, Pierre Van Delft^a, Didier Thoraval^a, François Doignon^a, Frédéric Domergue^a, Peter Luemmen^b and Jérôme Joubès^{a,1}

^a Univ. Bordeaux, CNRS, LBM, UMR 5200, F-33140 Villenave d'Ornon, France

^b Bayer AG, Research & Development, Crop Science, 65926 Frankfurt am Main, Germany

Corresponding Author : Jérôme Joubès, Laboratoire de Biogenèse Membranaire, UMR5200, CNRS- université de Bordeaux, Bâtiment A3, INRAE Bordeaux Aquitaine, 71 Avenue Edouard Bourlaux, CS 20032, F-33140 Villenave d'Ornon, France, Email : jerome.joubes@u-bordeaux.fr

¹ The author responsible for distribution of materials integral to the findings presented in this article in accordance with the policy described in the Instructions for Authors is Jérôme Joubès (jerome.joubes@u-bordeaux.fr)

ABSTRACT

Very-long-chain fatty acids (VLCFA) serve as precursors for various lipids that play crucial physiological and structural roles in plants. The β -keto-acyl-CoA synthase (KCS) catalyzes the initial step of VLCFA elongation and determines the chain-length substrate specificity of the fatty acid elongase complex. Following an extensive phylogenetic analysis, 28 KCS genes from various plant species, including 17 functionally uncharacterized genes, were expressed in *Saccharomyces cerevisiae*, and their VLCFAs profiles were analyzed using gas chromatography-mass spectrometry. Yeast expressing active KCS were subsequently exposed *in vivo* to various Group 15 herbicides to investigate their mode of action and selectivity. These experiments revealed differential sensitivities of KCS enzymes to benfuresate, cafenstrole, flufenacet, pyroxasulfone, and metazachlor, while endogenous VLCFA synthesis in yeast, which relies on Elop-type elongases, remained unaffected. Furthermore, to address a significant gap in understanding the inhibitory potency of Group 15 herbicides, we developed an *in vitro* enzymatic assay based on the quantification of the 3-oxo-products generated during the KCS-catalyzed reaction using high-performance liquid chromatography-mass spectrometry coupled with UV detection. This

1
2
3 1 novel biochemical approach enabled the evaluation of inhibitor potency as well as the kinetic
4 2 characterization of both established and newly identified KCS enzyme inhibitors.

5
6
7 3 Keywords : KCS, herbicides, plant, yeast, acyl-CoA

8 9 10 4 **1. Introduction**

11
12
13
14 5 Very-long-chain fatty acids (VLCFAs), which consist of 20 or more carbon atoms, are essential
15 6 molecules with critical physiological and structural roles in most organism [1]. In plants, VLCFAs are
16 7 integral components of key lipids, including phospholipids and sphingolipids, seed triacylglycerols,
17 8 cuticular waxes, and root suberin [2,3]. They are synthesized in the endoplasmic reticulum (ER) via the
18 9 activity of a multi-enzymatic fatty acid elongase (FAE) complex. The core FAE complex comprises four
19 10 main enzymes that catalyze the sequential addition of a C2 unit from malonyl-CoA to the growing acyl
20 11 chain. The first and rate-limiting step involves the condensation of the acyl-CoA substrate (n) with
21 12 malonyl-CoA to produce 3-oxo-acyl-CoA (n+2), a reaction catalyzed by the β -keto-acyl-CoA synthase
22 13 (KCS). This intermediate is subsequently reduced by the β -keto-acyl-CoA reductase (KCR) to yield 3-
23 14 hydroxy-acyl-CoA, which is then dehydrated by the 3-hydroxy-acyl-CoA dehydratase (HCD) to form
24 15 enoyl-CoA. Finally, the enoyl-CoA reductase (ECR) reduces the enoyl-CoA to generate an acyl-CoA that
25 16 is two carbons longer (n+2) than the original substrate. This elongation cycle is repeated to produce
26 17 VLCFAs with chain lengths ranging from C20 to C38 or even longer.

27 18 Although the structure of the elongase complex remains poorly understood, it is now widely accepted
28 19 that multiple elongases coexist in plant cells to generate VLCFAs of varying chain lengths. KCS plays a
29 20 pivotal role by catalyzing the rate-limiting step of the elongation reaction and defining both substrate
30 21 specificity and tissue-specific elongation of fatty acids. Consequently, over 20 KCS isoforms have been
31 22 identified in the genome of various angiosperms: 21 in Arabidopsis [4], 24 in grapevine [5], 25 in
32 23 sorghum [6], 26 in maize [7], 22 in rice [8,9], and as many as 58 in cotton and rapeseed [10,11]. In
33 24 contrast, KCR, HCD, and ECR, encoded by one or two genes, exhibit broad substrate specificity, are
34 25 expressed ubiquitously and are shared by all FAE complexes [12,13,14,15].

35 26 The KCS gene family in *Arabidopsis thaliana* has been particularly well studied, however the precise
36 27 biochemical activities and physiological roles of several Arabidopsis KCS isoforms remain unresolved
37 28 [3,16]. Despite their high sequence homology, phylogenetic analyses have allowed the classification
38 29 of Arabidopsis KCS proteins into eight clades, α to θ [4]. If the yeast *Saccharomyces cerevisiae* has been

1
2 1 widely used in previous studies as a heterologous system, only 12 of the 21 Arabidopsis KCS isoforms
3
4 2 (KCS1, KCS2, KCS3, KCS4, KCS5, KCS6, KCS9, KCS10, KCS16, KCS17, KCS18, KCS20) have been
5
6 3 functionally characterized in this system [17,18,19,20,21,22,23,24]. Collectively, these studies suggest
7
8 4 that KCS enzymes from the same phylogenetic clade tend to exhibit similar chain-length specificities.
9
10 5 Although *in vitro* enzyme assays offer valuable insights into enzyme kinetics and inhibition
11
12 6 mechanisms, the membrane association of KCS enzymes complicates their recombinant functional
13
14 7 expression and purification. Nevertheless, a few studies have confirmed KCS activities, including
15
16 8 substrate specificity, through *in vitro* assays using ¹⁴C-radiolabeled substrates and microsomal
17
18 9 fractions from genetically modified yeast strains [18,25,26] or purified recombinant KCS expressed in
19
20 10 yeast [27,28].

21
22 11 The Herbicide Resistance Action Committee (HRAC) classifies herbicides according to their modes of
23
24 12 action, target sites, symptoms, and chemical classes. Group 15 herbicides have been initially grouped
25
26 13 based on biological symptoms and physiological studies demonstrating inhibition of VLCFA
27
28 14 biosynthesis. Notably, Group 15 herbicides effects on Arabidopsis KCS enzymes expressed in yeast,
29
30 15 has been studied *in vivo*, revealing significant inhibition of KCS1, KCS2, KCS5, KCS6, KCS18, and KCS20
31
32 16 by structurally diverse herbicides such as metazachlor, flufenacet, and cafenstrole at concentrations
33
34 17 of 1 or 100 μ M [17,19]. Other Group 15 herbicides, such as alachlor, anilofos, and fentrazamide, have
35
36 18 shown differential inhibition of specific KCS isoforms [17]. A recent study examined the effects of
37
38 19 Group 15 herbicides on *Populus trichocarpa* KCS1, KCS2 and KCS4 enzymes expressed in yeast,
39
40 20 revealing that the degree of inhibition varied among the three paralogs, with fentrazamide and
41
42 21 flufenacet showing the strongest inhibitory effects on KCS enzymatic activity compared to the weaker
43
44 22 effects of alachlor and anilofos [29]. Previously, using a cell-free *in vitro* assay with microsomes from
45
46 23 *Allium porum* and ¹⁴C-radiolabeled substrates, the enzymatic target of the chloroacetamide
47
48 24 metazachlor has been identified as the condensation step in VLCFA biosynthesis [30]. Inhibition of
49
50 25 elongation reactions by the isoxazoline pyroxasulfone has also been demonstrated *in vitro* using a
51
52 26 recombinant rice KCS protein produced in *E.coli* or microsomes from rice cultured cells [31,32].

53 27 These findings highlight the complexity of Group 15 herbicide action, linked to the diversity of Group
54
55 28 15 chemotypes, as well as the challenges posed by the diversity of KCS isoforms and their substrate
56
57 29 specificities in different plant species. Notably, the low incidence of VLCFA biosynthesis inhibitors on
58
59 30 several weeds has been demonstrated [33]. Several factors may contribute to this resistance, including
60
61 31 the low frequency of mutations in condensing enzymes involved in VLCFA biosynthesis [17,31], as well

1
2
3 1 as the genetic redundancy of fatty acid elongases [21]. A better understanding of the mode of action
4 2 and chemical properties of herbicides targeting the VLCFA synthesis is therefore necessary to pave the
5
6 3 way for improved selectivity and reduced environmental impact.

7
8 4 In this study, we conducted a phylogenetic and functional analysis of KCS enzymes from various plant
9
10 5 species in order to evaluate if KCS enzyme activities, within the same evolutionary lineage, are
11
12 6 conserved across species. Additionally, we exposed yeast expressing active KCS enzymes to a range of
13
14 7 Group 15 herbicides to explore their mode of action and selectivity. Furthermore, we developed a
15
16 8 non-radioactive activity *in vitro* assay based on mass-spectrometric measurement of product
17
18 9 formation. This assay was successfully applied to characterize the inhibition of recombinantly
19
20 10 expressed KCS isoforms from different plant species by selected Group 15 herbicides.

23 11 **2. Methods**

24
25
26 12 **2.1. Chemical compounds.** Alachlor, benfuresate, flufenacet, metazachlor, and prosulfocarb
27
28 13 compounds were acquired from Sigma-Alrich (Saint-Louis, USA). Pyroxasulfone was obtained from
29
30 14 Combi-Blocks and cafenstrole from Atlantic Research Chemicals Ltd. Dimesulfazet, perfluidone, and 2-
31
32 15 hydroxybenfuresate were synthesized at Bayer, Crop Science Division (Frankfurt am Main, Germany).
33
34 16 Prosulfocarb sulfoxide was obtained as an analytical standard from Biomol GmbH (Hamburg,
35
36 17 Germany). Stock solutions of these compounds at 100 mM were prepared in DMSO.

37
38
39 18 **2.2. Phylogenetic analysis of plant KCS enzymes.** Protein sequences of the KCS from six
40
41 19 monocotyledonous and five dicotyledonous plant species were gathered from UniProt.
42
43 20 Monocotyledonous species included *Setaria italica* (Si), *Setaria viridis* (Sv), *Zea mays* (Zm), *Oryza sativa*
44
45 21 (Os), *Sorghum bicolor* (Sb), *Triticum aestivum* (Ta). Dicotyledonous species comprised *Arabidopsis*
46
47 22 *thaliana* (At), *Solanum lycopersicum* (Sl), *Vitis vinifera* (Vv), *Capsella rubella* (Cr), and *Brassica napus*
48
49 23 (Bn). Additionally, algae species included *Raphidocelis subcapitata*, *Chlamydomonas reinhardtii*, and
50
51 24 *Volvox carteri*. MUSCLE alignment of the protein sequences was performed using MEGA11 software,
52
53 25 and a maximum likelihood tree with 500 bootstraps was constructed.

54
55 26 **2.3. Generation of TRIPLE and TRIPLE *elo3Δ* yeast strains using CRISPR-Cas9.** Following the CRISPR-
56
57 27 Cas9 method described in [21], coding sequences of Arabidopsis genes *KCR1*, *PAS2*, and *ECR* were
58
59 28 successfully introduced into the *Saccharomyces cerevisiae* genome. These genes replaced the coding
60
61 29 sequences of *IFA38*, *PHS1* and *TSC13* respectively, resulting in the creation of the TRIPLE yeast strain.

1
2
3 1 The TRIPLE strain was further modified by deleting the endogenous yeast *ELO3* gene, producing the
4
5 2 TRIPLE *elo3Δ* strain.
6

7
8 **2.4. Construction and transformation of DNA constructs for heterologous expression in yeast.** Non-
9
10 4 Arabidopsis DNA fragments were synthesized by AZENTA (Burlington, MA, USA) and Invitrogen
11
12 5 (Waltham, MA, USA) in the destination vectors pU-GW-Kan and pDONR221, respectively (**Table S1**).
13
14 6 These fragments were transferred into the pVT-Leu DESTINATION vector [34,35] using LR clonase
15
16 7 (Invitrogen). TRIPLE and TRIPLE *elo3Δ* yeast cells were transformed with these constructs following
17
18 8 the standard lithium acetate transformation protocol [36] and grown on SD-L solid medium (Synthetic
19
20 9 Defined Medium minus leucine). Yeast cells were transformed with constructs as described in [21].
21

22
23 **2.5. Heterologous expression and inhibition of plant VLCFA elongases in yeast.** Transformed yeast
24
25 11 cells from various strains are derived from the INVSc1 genetic background (Invitrogen) were grown for
26
27 12 72 hours at 30°C in 1mL of SD-L liquid medium with 2% glucose. The cells were then pelleted and
28
29 13 washed with 1 mL of distilled water. Fatty acid composition was analyzed (see Fatty Acid Methyl Esters
30
31 14 (FAME) preparation and analysis) and compared with that of cells transformed with empty pVT-Leu
32
33 15 vector as control. When elongase activity was observed, inhibition experiments were conducted by
34
35 16 adding herbicides to final concentrations of 1mM, 10mM or 100 M at the time of induction in a fresh
36
37 17 1-ml culture. After 72 hours of incubation, cells were processed as described above, and fatty acid
38
39 18 composition was compared with that of cells expressing the same KCS grown in the absence of
40
41 19 herbicide. Strain growth analyses were performed using a SPECTROstar Nano microplate reader (BMG
42
43 20 LABTECH, Champigny sur Marne, France), maintained at 30 °C. Yeast growth was monitored by
44
45 21 measuring the turbidity at OD600 every 30 minutes.

46
47 **2.6. Microsomal fraction preparation (Adapted from [37] and [38]).** Yeast transformants were initially
48
49 23 grown in 2 mL of SD-L liquid medium with 2% glucose for 24 hours at 30°C. Subsequently, the cells
50
51 24 were transferred to 100 mL of fresh medium and grown for 24 h at 30 °C, aiming for a final OD600 of
52
53 25 6 to 10. Yeast cells were harvested (6,000 g for 5 minutes at 4 °C), washed with ice-cold 20 mM Tris
54
55 26 HCl (pH 7.9), and centrifuged again (6,500 g for 10 minutes at 4 °C). The resulting pellets were
56
57 27 resuspended in lysis buffer containing 20 mM Tris HCl (pH 7.9), 10 mM MgCl₂, 1 mM EDTA, 5% (vol/vol)
58
59 28 glycerol, 1 mM DTT and 0.3 M ammonium sulfate. Cell disruption was achieved using glass beads (710-
60
61 29 1180 μm) with a QIAGEN Tissue Lyser. The lysate was recovered from glass beads, and cell debris were
62
63
64
65

1 removed by centrifugation (6,500 g for 10 minutes at 4 °C). The supernatant was further centrifuged
2 at 110,000 g for 2 hours at 4 °C (Sorval/TH641). The resulting microsomal membrane pellets were
3 suspended in 0.5 mL of storage buffer containing 50 mM HEPES (pH 6.8), 1mM DTT, and 2% glycerol.
4 Protein concentrations were determined using the Bio-Rad protein assay reagent. All these steps were
5 performed on ice or at 4°C. The microsomal suspensions were stored at -70 °C until enzyme assays
6 were conducted.

7 **2.7. Fatty Acid Methyl Esters (FAME) preparation and analysis.** FAMES were obtained by
8 transmethylation at 85°C for 2 hours in 1mL of 0.5 M sulfuric acid in methanol containing 2% (v/v)
9 dimethoxypropane and 20 µg of heptadecanoic acid (C17:0) as an internal standard. After cooling, 1
10 mL of 2.5% (w/v) NaCl was added, and the FAME molecules were extracted in 300 µL of hexane for
11 subsequent analysis using a gas chromatograph (7890A, Agilent, Waldbronn, Germany) equipped with
12 an HP-5MS column (30 m x 0.25 mm x 0.25 mm, Agilent) coupled with mass spectrometry (MS) (5975B
13 insert MSD, Agilent, Waldbronn, Germany). The initial temperature was set to 50°C for 1 minute, then
14 increased at 25°C.min⁻¹ to 210°C, followed by an increased at 10°C.min⁻¹ to 306°C, then at 65°C.min⁻¹
15 to 320°C, and finally held for 3 minutes at 320°C, with helium as carrier gas, for a total run time of 21
16 minutes. Data collection and processing were performed using Agilent MassHunter software. The
17 proportion of each FAME was calculated based on individual and total peak areas of the FAMES.
18 Quantitative analyses were conducted using an Agilent 7890A gas chromatograph equipped with an
19 Agilent HP-5MS column and flame ionization detector. The same GC program was used, with hydrogen
20 (1.5 mL.min⁻¹) as the carrier gas. Acyl chain quantities were determined relative to the intensity of the
21 peak associated with the quantity of heptadecanoic acid (C17:0).

22 **2.8. KCS enzymatic activity and inhibition by herbicides.** KCS enzymatic activity was measured in a
23 100 µL reaction mixture containing 20 to 60 µg of microsomal fraction, 10 mM phosphate sodium
24 (Na₂HPO₄) buffer (pH 6.8), 100 µM malonyl-CoA, 100 µM acyl-CoA, and 2% DMSO. The reaction was
25 conducted at 30 °C for 30 minutes. Inhibitor response curves of KCS enzymes were generated in the
26 presence of increasing concentrations of herbicides prepared in DMSO. For pre-incubation
27 experiments, microsomes were incubated at 30°C for 15 minutes in presence of the inhibitor and in
28 absence of the substrates. The reaction was initiated by adding 100 µM malonyl-CoA and 100 µM acyl-
29 CoA in NaH₂PO₄ buffer (pH 7.2) and incubated at 30°C for 30 minutes. The reaction was then stopped
30 by adding 200 µL of methanol, followed by a 30-second vortexing step. The samples were then

centrifuged at 13,000 g for 2 minutes, and the supernatant was transferred into vials for HPLC-UV-MS/MS analysis.

2.9. HPLC-UV-MS/MS analysis. The HPLC-MS/MS analysis was performed using a Waters Acquity UPLC H-Class system coupled with a Waters ACQUITY UPLC Tunable UV detector at 260 nm. Separation was achieved on a Kinetex C18 5 μ m chromatographic column (100 mm x 2.1 mm, 100 Å, Phenomenex) and an ACQUITY UPLC CSH C18 VanGuard precolumn (5 mm x 2.1 mm, 1.7 μ m, 130 Å) (Waters, Milford, MA, USA). The mobile phase A consisted of 10 mM ammonium acetate in water at pH 8.5 and the mobile phase B was acetonitrile. Gradient elution (0.0 min, 40% B; 8 min, 95% B; 8.50 min, 95% B; 9 min, 40% B; 12 min, 40% B) was performed at a flow rate of 0.3 mL/min, with an injection volume of 10 μ L, and a constant column temperature of 35 °C. Acyl-CoA detection was conducted using a Waters Xevo TQ-S micro mass spectrometer operated with an ESI probe. Positive electrospray ionization (5500 V) was applied, using nitrogen as desolvation and nebulizing gas, while argon was used as the collision gas for fragmentation. The source and desolvation temperatures were set at 150 and 350 °C, respectively. The gas flow to the cone was adjusted at 1 L.h⁻¹ and the gas desolvation flow at 750 L.h⁻¹. Ion transitions, retention times, and compound-specific parameters for all acyl-CoAs are summarized in **Table S2**. Data was collected and processed by MassLynx 4.1 software.

2.10. Statistical analysis. Tukey's post hoc test was performed using RStudio to assess statistically significant differences in KCS activity. The Student's t-test was used to evaluate the herbicide effect. The reported values represent means \pm standard deviations (SD).

3. Results

3.1. Phylogenetic analyses of the plant KCS family

A rooted comparative phylogenetic tree was constructed based on a MUSCLE alignment of 362 KCS proteins from 14 species, including algae, monocotyledonous and dicotyledonous plants (**Figure 1**). Algae species were represented by 13 KCS from *Raphidocelis subcapitata* (annotated RsKCS), 1 from *Chlamydomonas reinhardtii* (CreKCS, [39]) and 1 from *Volvox carteri* (VcarKCS, [39]). Monocotyledonous species were *Setaria italica* (30 SiKCS), *Setaria viridis* (30 SvKCS), *Zea mays* (28 ZmKCS, [7,40]), *Oryza sativa Japonica* (22 OsKCS, [8]), *Oryza sativa Indica* (32 OsKCS), *Sorghum bicolor* (25 SbKCS, [6]), and *Triticum aestivum* (39 TaKCS). Dicotyledonous species were *Arabidopsis thaliana*

(21 AtKCS, [4]), *Solanum lycopersicum* (19 SlKCS), *Vitis vinifera* (24 VvKCS, [5]), *Capsella rubella* (21 CarubKCS/CrKCS), and *Brassica napus* (58 BnKCS, [11]). As shown in **Figure 1**, the phylogenetic tree of the plant KCS family revealed 12 distinct clades, including the 8 clades previously described for Arabidopsis (clades α to θ) [4], the 3 monocot-specific clades previously described (ι , κ , and λ) [7], and one algae-specific subgroup. The κ clade contained the highest number of sequences (73), followed by θ (53), ζ (45), ι (28), α (25), λ (24), γ (23), δ (22), ϵ (22), β (20) and η (11). Among the 3 monocot-specific, the κ and ι clades exclusively comprised KCS proteins from the monocot species studied here, while the λ group predominantly contained monocot KCS proteins but also included a few KCS proteins from the dicots *Vitis vinifera* and *Solanum lycopersicum*. The first eight groups (α , β , γ , δ , ϵ , ζ , η , and θ) were previously designated as KCS4/9/17-like (α), FAE1-like (β), CER6-like (γ), KCS1-like (δ), KCS2/20-like (ζ), KCS10/FDH-like (ϵ), KCS7/21-like (η), and KCS3/12/19-like (θ) [4]. In our analysis, the β and η clades appear to be dicot-specific. Interestingly, in the six clades that include both dicot and monocot KCS proteins (α , γ , δ , ζ , ϵ and θ), KCS from each flowering plant group are distinctly separated. This observation suggests a divergent evolutionary trajectory of KCS families in monocots and dicots following the emergence of monocotyledonous plants [5,8,39].

3.2. Functional characterization of a set of plant KCS in yeast

To investigate the substrate specificity divergence of KCS enzymes, KCS condensation activity was evaluated through heterologous expression in yeast, followed by fatty acid methyl ester (FAME) analysis. Yeast naturally synthesizes VLCFAs (predominantly C26:0, with minor levels of C20:0 and C20:1) due to the activity of its native Elo2p and Elo3p enzymes, which lack sequence similarity with KCSs. Notably, Elo3p catalyzes the elongation of C22 to produce C24 and C26 VLCFAs so that the *elo3 Δ* mutant accumulates C22 VLCFAs [41]. KCS genes were expressed in the two distinct yeast backgrounds previously used allowing the reconstitution of the entire plant FAE complexes [21]: the TRIPLE strain, in which the yeast FAE core subunits (*IFA38*, *PHS1*, and *TSC13*) were replaced by their *Arabidopsis* orthologs (*KCR1*, *PAS2*, and *CER10*), and the TRIPLE *elo3 Δ* strain which incorporates the same modifications as the TRIPLE strain but includes in addition a deletion of the *ELO3* gene, leading to the accumulation of C22 VLCFA precursors. KCS activity was detected as an increase in VLCFA accumulation relative to the empty vector yeast strain. A total of 28 KCS enzymes from six different phylogenetic clades (**Figure 2A**) were expressed in both yeast strains, and the resulting VLCFA profiles were analyzed using gas chromatography-mass spectrometry (GC-MS) (**Figures 2B and 2C**). The

1
2
3 1 selected KCS included nine and two functionally characterized condensing enzymes from *Arabidopsis*
4 2 *thaliana* [21] and *Zea mays* [7], respectively. All 17 previously uncharacterized KCS enzymes were
5
6 3 found to be enzymatically active in one or both strains. For clarity, **Figure 2** reports only the most
7
8 4 suitable yeast strain for characterizing the activity of each KCS enzyme.

9
10 5 From the α clade, 14 active KCS enzymes from 9 different species were analyzed. Upon expression of
11
12 6 these enzymes in the TRIPLE *elo3Δ* yeast strain, VLCFA profiles similar to those of either AtKCS4,
13
14 7 AtKCS9, or AtKCS17 were obtained. The Arabidopsis α clade is characterized by high sequence
15
16 8 similarity and overlapping substrate specificities, as exemplified by AtKCS4, AtKCS9 and AtKCS17,
17
18 9 which share 66% to 98% sequence identity. All three enzymes elongate C22 to produce C24 and C26
19
20 10 VLCFAs, but with distinct C24:C26 ratios [21]. The AtKCS4-like VLCFA profile, characterized by a
21
22 11 significant C26 accumulation, was observed for both dicot (e.g., SlKCS4, CrKCS4) and monocot (e.g.,
23
24 12 ZmKCS4, ZmKCS15, SvKCS4, SbKCS18) KCSs (**Figure 2B**). The AtKCS9-like profile, characterized by high
25
26 13 C24 accumulation with minor C26 levels, was observed for the monocot CrKCS9 and the dicot
27
28 14 BnKCS31. The substrate specificity of AtKCS17, characterized by prominent C24 accumulation, was
29
30 15 observed for the dicot CrKCS17. However, the wheat TaKCS4 and the grape VvKCS10 did not match
31
32 16 the profiles of AtKCS4, AtKCS9, or AtKCS17, despite sharing 75–82% sequence identity. Instead,
33
34 17 TaKCS4 exhibited high C20:1 accumulation, resembling the AtKCS18 VLCFA profile from the β clade,
35
36 18 which is phylogenetically related to the α clade (**Figure 2B**). VvKCS10 led to significant C22:0
37
38 19 accumulation when expressed in the TRIPLE strain compared to the control strain (**Figure 2C**). In our
39
40 20 phylogenetic analysis, two KCSs from *Sorghum bicolor* and *Vitis vinifera* were assigned to the γ clade,
41
42 21 represented by AtKCS5 and AtKCS6 (**Figure 2A**). However, their substrate specificities differed from
43
44 22 those of these Arabidopsis KCSs (**Figure 2B**). SbKCS6 expression resulted in high C20:1 accumulation,
45
46 23 similar to AtKCS18 (**Figure 2C**), while VvKCS16 exhibited a VLCFA profile resembling that of AtKCS20,
47
48 24 with significant C22 and C24 accumulation. In the ζ/ι group, represented by AtKCS2 and AtKCS20
49
50 25 (**Figure 2A**) which share 85% sequence identity, elongation profiles remained consistent with C22
51
52 26 accumulation [21]. Six KCS enzymes from these clades, including dicot (BnKCS38 and VvKCS5) and
53
54 27 monocot (TaKCS2, TaKCS20 and OsKCS2) KCSs, were analyzed. Both dicot BnKCS38 and monocot
55
56 28 TaKCS20 produced KCS2-like VLCFA profile with significant C22 accumulation. TaKCS2 exhibited an
57
58 29 AtKCS20-like profile, with minor C24 accumulation. In contrast, OsKCS2 from the ι group (65–67%
59
60 30 identity with AtKCS2/20) differed with a VLCFA profile with high C26:0 accumulation in the TRIPLE
61
62 31 strain (**Figure 2C**). Finally, RskCS1 and RskCS2 from the green algae *Raphidocelis subcapitata* shared

only 50% sequence identity with AtKCS2 and AtKCS20 but exhibited similar substrate specificities. These enzymes catalyzed the C22 accumulation, as AtKCS2 and AtKCS20, while also promoting the C20:0 accumulation in the TRIPLE *e/o3Δ* strain. Overall, these results align with previous studies on Arabidopsis KCS enzymes, and confirm that enzyme activities are broadly conserved within the phylogenetic clades previously identified [4,17,19].

3.3. Inhibition of activity of different plant KCSs by a set of herbicides

To investigate the mode of action of herbicides from HRAC Group 15, the 28 transgenic yeast strains expressing these active KCS enzymes were incubated in the presence of five herbicides of different chemotypes: the benzofuran benfuresate, the azolylcarboxamide cafenstrole, the α -oxyacetamide flufenacet, the α chloroacetamide metazachlor and the isoxazoline pyroxasulfone, at an initial concentration of 10 μ M. These five herbicides are widely used and have already been extensively tested on Arabidopsis KCS enzymes. Yeast cell growth was not affected during the incubation period by any of the herbicides, as monitored through yeast growth curves with and without the inhibitors (**Figure S1A and B**). Furthermore, the synthesis of endogenous VLCFAs by the yeast Elop enzymes was not inhibited, as the endogenous fatty acid levels in TRIPLE and TRIPLE *e/o3Δ* strains transformed with empty vector remained unchanged upon the addition of any of the herbicides (**Figure S1C**). The effects of these herbicides on KCS activity were quantified as the relative percentage accumulation of the main VLCFA product compared to the control treatment (**Figure 3**). While benfuresate induces the characteristic fiddlehead phenotype in plants, it does not inhibit Arabidopsis KCSs. This lack of inhibition may be due to limited bio-activation or bioavailability in yeast [17]. Thus, benfuresate did not inhibit any of the 28 KCS expressed in yeast, as shown by approximately 100% VLCFA accumulation relative to the control treatment (**Figure 3**). In contrast, the four other herbicides significantly inhibited most of the expressed KCS enzymes at 10 μ M. In most cases, treatment with cafenstrole, flufenacet, metazachlor, or pyroxasulfone drastically reduced the amount of VLCFAs produced by the FAE complex. For instance, treatments of AtKCS4 expressing yeast with cafenstrole, flufenacet, metazachlor and pyroxasulfone reduced significantly the amounts of the C24 product, which represented only 11%, 14%, 22% and 12%, respectively, of the C24 content observed in the control treatment (**Figure 3**). Conversely, the same treatments induced a marked increase in the accumulation of the C22 substrate, resulting in C22 accumulation 566%, 618%, 484% and 609% higher, respectively, relative to the control treatment (data not shown). In rare cases, inhibition was not statistically

1
2
3 1 significant. For example, yeast expressing SIKCS4 treated with cafenstrole and metazachlor showed
4 2 48% and 72% of C24 accumulation, respectively, compared to the control treatment. Similarly,
5
6 3 SbKCS18 expressing yeast showed 52% of C24 accumulation with metazachlor, and TaKCS20 exhibited
7
8 4 40% of C24 accumulation with pyroxasulfone, relative to the control treatment.

9
10 5 Altogether these analyses showed that cafenstrole, flufenacet, metazachlor, and pyroxasulfone
11
12 6 effectively reduced VLCFA accumulation in yeast transformed with plant KCSs, while benfuresate,
13
14 7 which had no inhibitory effect on any of the KCS enzymes tested. In addition, they suggest that none
15
16 8 of the inhibitors tested in this study appeared specific for KCS enzymes based on their plant origin or
17
18 9 substrate preference. These results therefore suggest herbicide-specific interactions with the
19
20 10 condensing enzymes but no specificity based on the plant origin of the KCS genes.

21 22 23 11 **3.4. Development of a biochemical *in vitro* assay to quantify the 3-oxo-products of the KCS-catalyzed** 24 25 12 **reaction**

26
27 13 The fatty acid elongation cycle begins with the KCS-catalyzed condensation of malonyl-CoA and acyl-
28
29 14 CoA, resulting in the formation of a 3-oxo-acyl-CoA intermediate. Recently, the binding of 3-oxo-C20:0-
30
31 15 CoA to mammalian VLCFA elongases (ELOVL1-7), which share the same condensation activity as plant
32
33 16 KCSs, was examined [42]. A schema illustrating a ping-pong mechanism for ELOVL activity has been
34
35 17 proposed (**Figure 4A**). The acyl group is transferred from acyl-CoA onto a cysteine residue (C residue)
36
37 18 in the KCS catalytic site. The decarboxylation of the malonyl-CoA, facilitated by the catalytic histidine
38
39 19 and asparagine residues (H and N residues), releases a molecule of CO₂. The nucleophilic attack of the
40
41 20 carbanion intermediate on the C1 of the thio-acyl intermediate produces and releases the 3-oxo-acyl
42
43 21 product. Based on this, it is assumed that 3-oxo-acyl-CoA is generated through a similar reaction
44
45 22 mechanism by plant KCSs [16]. However, 3-oxo-acyl-CoA, which is an inherently unstable intermediate
46
47 23 in the FAE reaction, is present in minimal quantities and therefore poorly characterized. Nevertheless,
48
49 24 in the absence of NADPH, its *in vitro* reduction by the β -ketoacyl-CoA Reductase (KCR), which uses
50
51 25 pyridine nucleotides (NADPH) as reductant, is prevented, causing the accumulation of the direct
52
53 26 product of the KCS activity [14,26,28].

54
55 27 To further evaluate the sensitivity of the different KCS enzymes to these inhibitors, assays must be
56
57 28 conducted *in vitro* at increasing inhibitor concentrations, with quantification of the KCS reaction
58
59 29 product at each inhibitor concentration. As the product of KCS is an acyl-CoA, GC-MS analysis of total
60
61 30 FAMES does not directly reflect enzyme activity. Instead, combining UV detection with MS/MS analysis

1 enables the detection of acyl-CoA products. Specifically, high-performance liquid chromatography-
2 mass spectrometry coupled with UV detector (HPLC-UV-MS/MS) allows for the detection of acyl-CoA
3 thioesters, with UV absorbance at 260 nm providing an initial confirmation of their presence based on
4 characteristic absorbance features and MS/MS formerly identifying the acyl-CoA molecular species.
5 Product ion mass spectrum for 3-oxo-C20:0-CoA was acquired to determine the precursor and
6 production pairs to monitor (**Figure 4B, Table S2**). The most abundant fragment ion (m/z 570) was the
7 one formed by the neutral loss of the phosphorylated ADP moiety (M-507) from the precursor ion
8 (m/z 1077).

9 We therefore decided to set up an *in vitro* assay in the absence of NADPH using yeast microsomes
10 expressing KCS as enzyme source followed by HPLC-UV-MS/MS analysis to quantify 3-oxo-acyl-CoAs.
11 To calibrate the sensitivity of 3-oxo-C20:0-CoA quantification, nine standard solutions of 3-oxo-C20:0-
12 CoA, ranging from 17 to 2000 pmol, were analyzed. Using a 10 μ l injection loop, a calibration curve
13 was established based on the relationship between the response (peak area) and the quantity of 3-
14 oxo-C20:0-CoA in standard solutions (**Figure 4C**). The calibration curve further showed a coefficient of
15 determination (R^2) of 0.99 within a linear range from 17.5 to 500 pmol, underscoring the accuracy and
16 reliability of the method for quantifying 3-oxo-C20:0-CoA. The sensitivity of the method was evaluated
17 by determining the Limit of Detection (LOD) and Limit of Quantification (LOQ). The LOD and LOQ were
18 calculated by analyzing the signal-to-noise (S/N) ratio of low analyte quantities compared to the
19 baseline. The LOD was defined as the lowest quantity producing an S/N ratio greater than 3, while the
20 LOQ corresponded to the lowest quantity with an S/N ratio greater than 10. The LOD and LOQ were
21 found to be 0.05 pmol and 0.17 pmol, respectively.

22 We then used this set up to measure *in vitro* KCS enzymatic activities. First, yeast microsomes
23 expressing KCS enzymes were prepared and utilized to study the condensation activity of KCS using as
24 substrates acyl-CoA of different chain length. The *in vitro* condensation assay was performed with
25 malonyl-CoA and commercially available acyl-CoAs. To optimize the parameters for the *in vitro*
26 measurement of KCS activity, we evaluated reaction time and protein quantity. Experiments were
27 conducted with different reaction times (0, 15, 30, and 60 minutes at 30°C) and three different yeast
28 microsomal protein quantities (20 μ g, 40 μ g, and 60 μ g), using yeast TRIPLE *e/o3* Δ expressing AtKCS4 as
29 the enzyme source (**Figure S2**). C22:0 acyl-CoA, the preferred substrate of AtKCS4 [21], and malonyl-
30 CoA were used as substrates at a concentration of 100 μ M. The results indicated that a 30-minute
31 incubation was optimal for the KCS reaction, as the highest amount of 3-oxo-C24:0-CoA product was

1
2 1 detected at this time point when using 40 µg or 60 µg of microsomal protein. Based on these findings,
3
4 2 subsequent experiments were performed with a 30-minute reaction time and 40µg to 60µg of
5
6 3 microsomal proteins to ensure a sufficient signal for quantification.
7
8

9 4 **3.5. Flufenacet inhibits several microsomal KCS4-like enzymes**

10
11
12 5 The biochemical *in vitro* assay was then used to evaluate the sensitivity of KCS enzymes to inhibitors.
13
14 6 The activities of microsomal AtKCS4 and three AtKCS4-like enzymes (SvKCS4, SlKCS4, and SbKCS18),
15
16 7 which efficiently elongate C22:0 acyl-CoA into C24:0 acyl-CoA (**Figure 2**), were tested in the presence
17
18 8 of C22:0 acyl-CoA and malonyl-CoA as substrates and increasing concentrations of flufenacet, up to
19
20 9 100 µM. Flufenacet likely inhibits KCS through a nucleophilic reaction between the SH group of a
21
22 10 cysteine residue in the KCS active site (**Figure 5A**), a mechanism previously proposed for pyroxasulfone
23
24 11 and metazachlor in earlier studies [32,43]. The dose-response curves exhibited similar profiles for all
25
26 12 tested KCS enzymes, as reflected in their apparent IC₅₀ values, ranging from 9.12 10⁻⁷M to 79.8 10⁻⁷M
27
28 13 (**Figures 5B and 5C**), suggesting a common inhibitory mechanism across different paralogs and species.
29
30 14 To gain further insights into the flufenacet's mechanism of action, we examined whether the inhibition
31
32 15 of KCS reaction exhibited time dependency by pre-incubating the KCS expressing yeast microsomes
33
34 16 and the flufenacet before initiating the condensation reaction by adding the substrates. The dose-
35
36 17 response curves for the four tested KCS enzymes were impacted by the pre-incubation with the
37
38 18 inhibitor, as evidenced by differences in dose-response profiles and apparent IC₅₀ values between the
39
40 19 two conditions (with or without pre-incubation; **Figures 5B and 5C**). For all tested KCS, inhibition by
41
42 20 flufenacet was significantly more pronounced following a 15-minutes pre-incubation, suggesting that
43
44 21 flufenacet's mechanism of inhibition may be irreversible.
45
46 22

47 23 **3.6. Structurally diverse herbicides inhibit SvKCS4 *in vitro***

48
49
50 24 To evaluate the sensitivity of KCS to different inhibitors from Group 15 herbicides, the biochemical *in*
51
52 25 *vitro* assay was conducted using microsomes from yeast expressing SvKCS4. The enzyme activity was
53
54 26 quantified with increasing concentrations of various herbicide chemotypes, up to 100 µM. SvKCS4
55
56 27 expressing yeast microsomes were pre-incubated with the inhibitors for 15 minutes in the absence of
57
58 28 the C22:0-CoA substrate. Several herbicides from different chemotypes, including the α-
59
60 29 chloroacetamides, alachlor and metazachlor, the isoxazoline pyroxasulfone, the α-oxyacetamide
61
62
63
64
65

1 flufenacet, the azolylcarboxamide cafenstrole, the thicarbamates, prosulfocarb and prosulfocarb
2 sulfoxide, the trifluoromethylsulfonilides, dimesulfazet and perfluidone, and the benzofurans,
3 benfuresate and 2-hydroxybenfuresate, were tested.

4 The α -chloroacetamides, the pyroxasulfone, the flufenacet, the cafenstrole and the
5 trifluoromethylsulfonilides inhibited the formation of 3-oxo-C24:0-CoA in a concentration-
6 dependent manner. The apparent IC₅₀ values for these different inhibitors, ranging from 0.53 10⁻⁷M
7 to 4.2 10⁻⁷M, are summarized in **Table 1**. Interestingly, the thiocarbamate prosulfocarb and the
8 benzofuran compound benfuresate showed no inhibitory effect at concentrations up to 100 μ M (with
9 IC₅₀>10⁻⁴M). However, the sulfoxide derivative of prosulfocarb and the proposed 2-
10 hydroxybenfuresate metabolite were found to be potent inhibitors of SvKCS4 enzymatic activity with
11 apparent IC₅₀ of 2.1 10⁻⁷M and 0.2 10⁻⁷M, respectively.

Herbicide	Chemotype	IC50 [M]
alachlor	α -chloroacetamide*	4.20.10 ⁻⁷
metazachlor	α -chloroacetamide*	1.30.10 ⁻⁷
pyroxasulfone	isoxazoline*	0.53.10 ⁻⁷
flufenacet	α -oxyacetamide*	1.40.10 ⁻⁷
cafenstrole	azolylcarboxamide*	0.78.10 ⁻⁷
prosulfocarb	thiocarbamate*	> 10 ⁻⁴
prosulfocarb sulfoxide	thiocarbamate* (metabolite)	2.10.10 ⁻⁷
dimesulfazet	trifluoromethylsulfonilide**	1.10.10 ⁻⁷
perfluidone	trifluoromethylsulfonilide***	0.51.10 ⁻⁷
benfuresate	benzofurane*	> 10 ⁻⁴
2-hydroxybenfuresate	benzofurane* (metabolite)	0.20.10 ⁻⁷

Table 1. Inhibition of *Setaria viridis* KCS4 by structurally diverse herbicides. 3-oxo-C24:0-CoA formation was measured as a function of the herbicide concentration following 15-minute pre-incubation with the inhibitor in the absence of substrates. The enzymatic reaction was initiated by adding 100 μ M malonyl-CoA and 100 μ M C22:0-CoA in NaH₂PO₄ buffer (pH 7.2) and conducted at 30°C for 30 minutes. IC₅₀ values were calculated using SigmaPlot 14.5 (Alfasoft). Chemotypes were termed

1
2
3 1 according to: 2024 HRAC MoA Classification Scheme (<https://hracglobal.com/tools/2024-hrac-global-herbicide-moa-classification>)*, [48]**, and [19]***.

4. Discussion

4 Recent research on fatty acid elongation in plants suggests that multiple elongase complexes act sequentially and/or in parallel to generate the diverse range of VLCFAs found in plant species. Among these complexes, the condensing enzymes (KCS) are considered key determinants of spatial and substrate specificity [3]. Studies in *Arabidopsis* have revealed both functional redundancy and broad spatiotemporal expression among *KCS* genes. While more than half of the *Arabidopsis KCS* genes are expressed ubiquitously across plant tissues, others display restricted expression, primarily in reproductive organs [4].

Functional characterization in yeast has expanded our understanding of activity of several *AtKCS* proteins [17,18,19,21,28]. Notably, it has been demonstrated that nine *AtKCS* enzymes, *KCS1*, *KCS2*, *KCS4*, *KCS5*, *KCS6*, *KCS9*, *KCS17*, *KCS18*, and *KCS20*, produce distinct VLCFA profiles when expressed in yeast [21]. Similarly, five *ZmKCS* enzymes, when expressed in yeast, show unique catalytic specificities, with profiles resembling those of their *Arabidopsis* orthologs [7,44]. The functional characterization of 17 previously uncharacterized *KCS* enzymes from various monocot or dicot plant species aligns with these previous studies and confirms that *KCS* enzyme activities are broadly conserved within the same phylogenetic clades.

Heterologous expression in yeast has also already been employed to study *in vivo* how HARC Group 15 herbicides inhibit VLCFA elongation. Several herbicides, including metazachlor, flufenacet, and cafenstrole, strongly inhibit *AtKCS1*, *AtKCS2*, *AtKCS5*, *AtKCS6*, *AtKCS18*, and *AtKCS20* at micromolar concentrations [17,19,30]. Recent studies on *Populus trichocarpa KCS* enzymes (*PtKCS1*, *PtKCS2*, and *PtKCS4*) revealed differential inhibition by alachlor, anilofos, fentrazamide, and flufenacet, suggesting that even minor amino acid variations in *KCS* sequences can influence herbicide sensitivity [29]. Additionally, time-dependent inhibition assays have shown that *AtKCS18/FAE1* undergoes irreversible inhibition by metazachlor and pyroxasulfone, likely due to covalent binding of the inhibitor to the enzyme active-site cysteine [31,45]. Interestingly, pyroxasulfone was in contrast found to reversibly inhibit a VLCFA elongase in rice, highlighting species-specific differences in inhibition mechanisms.

Although these studies confirmed that herbicides target VLCFA elongation, their findings were indirect, as such approaches cannot precisely identify the herbicide's exact target or determine the

1 inhibitory potency (IC₅₀) of the tested molecules. To achieve this level of accuracy, *in vitro* assays are
2 required. To date, only a few studies have employed *in vitro* assays to investigate KCS enzymatic
3 activity and substrate specificity. These studies typically utilized ¹⁴C-radiolabeled substrates and
4 microsomes from KCS-expressing yeast or purified KCS enzymes as enzyme sources. The most
5 extensively characterized condensing enzyme *in vitro* is AtKCS18/FAE1, which preferentially elongates
6 C16:0-, C16:1-, C18:0-, and C18:1-CoAs, producing C20:1-CoA as the primary product and C22:1-CoA
7 as a minor product [18,25,26,27,28]. Following expression in yeast and enzyme purification, the
8 substrate preferences of three other AtKCS enzymes (AtKCS1, AtKCS11 and AtKCS17) was further
9 elucidated [28]. For instance, AtKCS1 exhibited high activity with C16:0-, C16:1-, C18:0-, and C20:0-
10 CoAs, while AtKCS17 showed a preference for saturated acyl-CoAs, with optimal activity up to C22.
11 However, none of these studies using *in vitro* approaches have investigated the inhibitory potential of
12 Group 15 herbicides on the activity of KCS enzymes.
13 Despite the valuable insights gained from *in vitro* assays, these methods present several challenges,
14 including the need for specialized equipment, radioactive waste management, and safety concerns.
15 To address these limitations, we developed, in this study, an optimized *in vitro* KCS assay, eliminating
16 the use of radiolabeled substrates. This assay specifically measures KCS activity, rather than the
17 activity of the entire FAE complex, by directly quantifying the enzyme's product, the 3-oxo-acyl-CoA
18 intermediate, using HPLC-UV-MS/MS. This new method proved to be a powerful tool for investigating
19 KCS activity across various plant species, providing direct insights into KCS kinetics and substrate
20 preferences when previous *in vivo* studies examined FAE complex activity indirectly through lipid
21 FAME quantification. Furthermore, this targeted *in vitro* assay was used to evaluate KCS inhibition by
22 Group 15 herbicides and to enhance our understanding of their mechanism of action. The small
23 reaction volume also makes it suitable for evaluating inhibitory molecules only available in limited
24 quantities, an important advantage when developing and testing novel compounds. Using yeast
25 strains expressing different KCS enzymes, we tested the species-specific inhibition of flufenacet. Our
26 results revealed time-dependent inhibition, demonstrating that flufenacet irreversibly inhibits KCS
27 activity. Furthermore, we found that flufenacet exhibits broad, non-selective inhibition of KCSs from
28 both monocot and dicot plants. However, SIKCS4 displayed lower sensitivity to flufenacet, as reflected
29 by its higher IC₅₀ value. This finding aligns with *in vivo* results obtained in the yeast expression system,
30 where SIKCS4 showed partial inhibition of its activity. Several HRAC Group 15 herbicides, representing
31 diverse chemotypes, have been identified as potent inhibitors of SvKCS4 and other KCS isoforms,

1
2 1 confirming earlier findings [17,19,31,46,47,48]. Our biochemical assay, based on the quantification of
3
4 2 the 3-oxo-products of the KCS reaction, enables both the assessment of inhibitor potency and the
5
6 3 kinetic characterization of established and novel KCS inhibitors. It should be noted that for covalent,
7
8 4 irreversible inhibitors, such as chloroacetamides, oxyacetamides, and isoxazolines, the measured IC₅₀
9
10 5 values (apparent IC₅₀ values) are highly dependent on the pre-incubation time. Nevertheless, these
11
12 6 values still provide useful relative estimates for comparing inhibitor potencies and evaluating the
13
14 7 inhibition of different KCS isoforms.

15
16 8 Previous studies have suggested that some HRAC Group 15 herbicides require metabolic activation to
17
18 9 effectively inhibit VLCFA biosynthesis [49,50]. For example, sulfur oxidation has been proposed as a
19
2010 key activation step for thiobencarb [51]. Our results for the chemically related thiocarbamate
21
2211 prosulfocarb confirm that sulfur oxidation is required for potent KCS inhibition. Similarly, the
23
2412 herbicidal efficacy of the benzofuran herbicides ethofumesate and benfuresate was shown to be
25
2613 higher in transgenic rice expressing human cytochrome P450 monooxygenases [52]. Increased
27
2814 oxidative deethylation (for ethofumesate) or hydroxylation (for benfuresate) has been identified as a
29
3015 bioactivation mechanism, yielding herbicidal 2-hydroxy-metabolites. The data presented in **Table 1**
31
3216 clearly demonstrate that benfuresate must be converted to its 2-hydroxy-metabolite to act as a potent
33
3417 inhibitor of SvKCS4 *in vitro*.

35
3618
3719 In summary, the study of fatty acid elongation in plants continues to reveal the complex and important
38
3920 roles of KCS enzymes in VLCFA biosynthesis. Functional characterization in Arabidopsis, maize, and
40
4121 other species has highlighted both the redundancy and specificity of KCS genes, while heterologous
42
4322 expression in yeast, and to a lesser extend radiolabeled based *in vitro* assays, have provided deeper
44
4523 insights into substrate preferences and enzymatic activity. In this study, we developed a radiolabel-
46
4724 free KCS assay to enhance the precision of inhibitor studies, particularly for HRAC Group 15 herbicides,
48
4925 which exhibit broad and, in some cases, irreversible inhibition of KCS activity. Our findings underscore
50
5126 the importance of metabolic activation in herbicidal efficacy and suggest that species-specific
52
5327 variations in KCS sensitivity may influence herbicide selectivity. These insights not only advance our
54
5528 understanding of VLCFA biosynthesis regulation but also offer valuable tools for future research into
56
5729 plant lipid metabolism and herbicide development.

58
59
6030 **CRedit authorship contribution statement**

J.J., F.D. and P.L. conceived the project, J.J., F.D., C.L. and P.L. designed the experiments, C.L, P.L., G.U., S.P., D.T., F.D, F.D. and J.J. performed the experiments, C.L., F.D., P.L. and J.J. wrote the article with contributions of all the authors.

Declaration of competing interest

All authors declare no conflicts of interest.

Acknowledgements

This work was supported by the Centre National de la Recherche Scientifique and the university of Bordeaux. This material is based upon work supported by the ANRT (Association nationale de la recherche et de la technologie) with a CIFRE fellowship granted to Claire Le Ruyet. Lipid analyses were carried out at the Metabolome facility of Bordeaux (<https://cgfb.u-bordeaux.fr/>). The Bordeaux Metabolome-Lipidome Facility-MetaboHUB is supported by a grant from ANR (no. ANR-11-INBS-0010).

Appendix A. Supplementary data

Supplementary data to this article can be found online

Table S1. Accession number list.

Table S2. MS/MS transitions in HPLC-UV-MS/MS.

Figure S1. Influence of herbicides on endogenous VLCFAs. A, B. Growth analysis of TRIPLE *elo3Δ* and TRIPLE *elo3Δ* expressing AtKCS4 yeast strains treated with different Group 15 herbicides (10μM). The data represent the average of four biological replicates. DMSO indicates the negative control treatment. Abbreviations for herbicides are as follows: MZ: metazachlor, FF: flufenacet, CF: cafenstrole, BF: benfuresate, PR: pyroxasylfone. **C.** FAME profiles of INVSc1, TRIPLE, TRIPLE *elo3Δ* and TRIPLE *elo3Δ* AtKCS4 yeast strains treated with different herbicides (10μM). The data represent the average of five biological replicates.

Figure S2. Optimization of incubation time and enzyme concentration for AtKCS4 condensation activity. The 3-oxo-C24:0-CoA product issued from the condensation between C22:0-CoA and malonyl-CoA was quantified. Different quantities of microsomal proteins (0, 20, 40, 60 μg) were

1 incubated with malonyl-CoA (100 μ M) and C22:0-CoA (100 μ M) in NaH₂PO₄ buffer (pH 7.2) at 30°C for
2 incubation times of 0, 15, 30 or 60 minutes. Activity values represent the results from three
3 independent experiments.

4 **Figure legends**

5 **Figure 1. Phylogenetic tree of KCS proteins from multiple species.** The phylogenetic analysis,
6 performed using the Maximum Likelihood method with 500 bootstraps, involved 362 KCS amino acid
7 sequences, with a total of 1527 positions in the final dataset. Evolutionary analyses were conducted
8 using MEGA11. Arabidopsis KCS enzymes (AtKCS) are highlighted in bold green letters, while the KCS
9 candidates further characterized in this study are highlighted in bold.

10 **Figure 2. Expression of KCS from various species in yeast induces over-production of VLCFAs. (A)** KCS
11 cladogram showing the phylogenetic relationship between the 28 proteins from different species
12 expressed in yeast. **(B, C)** FAME profiles obtained with the TRIPLE *elo3Δ* **(B)** or TRIPLE **(C)** yeast strains
13 expressing a set of 28 KCSs, compared to the yeast strain transformed with the empty vector.
14 Arabidopsis KCS are highlighted in bold. The color-coded areas represent similar VLCFA profiles. Each
15 FAME species, including saturated, mono-unsaturated and hydroxylated VLCFAs, is denoted by its
16 carbon chain length (C20 to C28). Data are expressed as mean values (percentage of total VLCFAs)
17 with standard deviation (SD, at least n = 4). Statistical significance was determined using a Tukey test
18 (*P < 0.05, **P < 0.01, ***P < 0.001, ****P < 1e-4).

19 **Figure 3. Differential inhibition of KCS enzymes by Group 15 herbicides.** Relative accumulation
20 percentages of VLCFA products were calculated as the percentage of VLCFAs synthesized by specific
21 KCS expressed in TRIPLE *elo3Δ* **(A)** or TRIPLE **(B)** yeast strains treated with herbicides (10 μ M),
22 compared to untreated yeast strains. Arabidopsis KCS enzymes are highlighted in bold. Data
23 represents the mean \pm SD of 3 biological replicates. Statistical significance was assessed using
24 Student's t-test (*P < 0.05, **P < 0.01, ***P < 0.001, ****P < 1e-4). Abbreviations for herbicides are
25 as follows: BF : benfuresate, CF : cafenstrole, FF : flufenacet, MZ : metazachlor, PR : pyroxasulfone.

26 **Figure 4. Mechanistic model and analytical validation of KCS activity. (A)** Suggested model of β -keto-
27 acyl-CoA synthase (KCS) ping-pong catalytic mechanism, modified from [16] and [41]. **(B)** Mass

spectrum of the 3-oxo-C20:0-CoA obtained with collision energy of 45 eV. **(C)** Calibration plot of 3-oxo-C20:0-CoA in water/methanol (1:2, v:v). Mean values are given with SD (n=2).

Figure 5. Inhibition of AtKCS4-like enzymes by flufenacet. **(A)** Proposed covalent mechanism of KCS inactivation by flufenacet. The nucleophilic thiol group of the catalytic triad cysteine reacts with the electrophilic carbon of the oxyacetamide moiety as described in [42]. The 2-hydroxy-5-(trifluoromethyl)-1,3,4-thiadiazole serves as the leaving group during the reaction. **(B)** Inhibitor response curves of AtKCS4-like enzymes in the presence of increasing concentrations of flufenacet. 3-oxo-C24:0-CoA formation was measured as a function of the herbicide concentration with (green) or without (black) a 15-minute pre-incubation of yeast microsomes and flufenacet in absence of substrates. The enzymatic reaction was initiated by adding 100 μ M malonyl-CoA and 100 μ M C22:0-CoA in NaH₂PO₄ buffer (pH 7.2) and conducted at 30°C for 30 minutes. KCS activity is represented as the percentage of 3-oxo-C24:0-acyl-CoA products synthesized by a given KCS expressed in TRIPLE *elo3Δ* yeast strain treated with herbicides, relative to the untreated yeast strain (DMSO). Data represent the mean \pm SE from 2 or 3 biological replicates. **(C)** Apparent IC₅₀ values (M) of SvKCS4, AtKCS4, SIKCS4 and SbKCS18 by flufenacet were calculated using GraphPad Prism 9.

References

- [1] L. Kyselová, M. Vítová, T. Řezanka. Very long chain fatty acids, Prog. Lipid Res. 87 (2022), 101180, <https://doi.org/10.1016/j.plipres.2022.101180>.
- [2] A.V. Zhukov, M. Shumskaya. Very-long-chain fatty acids (VLCFAs) in plant response to stress, Funct. Plant Biol. 47 (2020), 695–703, <https://doi.org/10.1071/FP19100>.
- [3] M. Batsale, D. Bahammou, L. Fouillen, S. Mongrand, J. Joubès, F. Domergue. Biosynthesis and Functions of Very-Long-Chain Fatty Acids in the Responses of Plants to Abiotic and Biotic Stresses, Cells 10 (2021), 1284, <https://doi.org/10.3390/cells10061284>.
- [4] J. Joubès, S. Raffaele, B. Bourdenx, C. Garcia, J. Laroche-Traineau, P. Moreau, F. Domergue, R. Lessire. The VLCFA elongase gene family in Arabidopsis thaliana: phylogenetic analysis, 3D modelling and expression profiling, Plant Mol. Biol. 67 (2008), 547, <https://doi.org/10.1007/s11103-008-9339-z>.
- [5] H. Zheng, Y. Liang, B. Hong, Y. Xu, M. Ren, Y. Wang, L. Huang, L. Yang, J. Tao. Genome-Scale Analysis of the Grapevine KCS Genes Reveals Its Potential Role in Male Sterility, Int. J. Mol. Sci. 24 (2023), 6510, <https://doi.org/10.3390/ijms24076510>.

- [6] A. Zhang, J. Xu, X. Xu, J. Wu, P. Li, B. Wang, H. Fang. Genome-wide identification and characterization of the KCS gene family in sorghum (*Sorghum bicolor* (L.) Moench), *PeerJ* 10 (2022), e14156, <https://doi.org/10.7717/peerj.14156>.
- [7] A.A. Campbell, K.E. Stenback, K. Flyckt, T. Hoang, M.A.D. Perera, B.J. Nikolau. A single-cell platform for reconstituting and characterizing fatty acid elongase component enzymes, *PLOS ONE* 14 (2019), e0213620, <https://doi.org/10.1371/journal.pone.0213620>.
- [8] L. Yang, J. Fang, J. Wang, S. Hui, L. Zhou, B. Xu, Y. Chen, Y. Zhang, C. Lai, G. Jiao, Z. Sheng, X. Wei, G. Shao, L. Xie, L. Wang, Y. Chen, F. Zhao, S. Hu, P. Hu, S. Tang. Genome-wide identification and expression analysis of 3-ketoacyl-CoA synthase gene family in rice (*Oryza sativa* L.) under cadmium stress, *Front. Plant Sci.* 14 (2023), <https://doi.org/10.3389/fpls.2023.1222288>.
- [9] U.M. Khan, I.A. Rana, N. Shaheen, Q. Raza, H.M. Rehman, R. Maqbool, I.A. Khan, R.M. Atif. Comparative phylogenomic insights of KCS and ELO gene families in Brassica species indicate their role in seed development and stress responsiveness, *Sci. Rep.* 13 (2023), 3577, <https://doi.org/10.1038/s41598-023-28665-2>.
- [10] G.-H. Xiao, K. Wang, G. Huang, Y.-X. Zhu. Genome-scale analysis of the cotton KCS gene family revealed a binary mode of action for gibberellin A regulated fiber growth, *J. Integr. Plant Biol.* 58 (2016), 577–589, <https://doi.org/10.1111/jipb.12429>.
- [11] Y. Xue, J. Jiang, X. Yang, H. Jiang, Y. Du, X. Liu, R. Xie, Y. Chai. Genome-wide mining and comparative analysis of fatty acid elongase gene family in *Brassica napus* and its progenitors, *Gene* 747 (2020), 144674, <https://doi.org/10.1016/j.gene.2020.144674>.
- [12] H. Zheng, O. Rowland, L. Kunst. Disruptions of the *Arabidopsis* Enoyl-CoA reductase gene reveal an essential role for very-long-chain fatty acid synthesis in cell expansion during plant morphogenesis, *Plant Cell* 17 (2005), 1467–1481, <https://doi.org/10.1105/tpc.104.030155>.
- [13] L. Bach, L.V. Michaelson, R. Haslam, Y. Bellec, L. Gissot, J. Marion, M. Da Costa, J.P. Boutin, M. Miquel, F. Tellier, F. Domergue, J.E. Markham, F. Beaudoin, J.A. Napier, J.D. Faure. The very-long-chain hydroxy fatty acyl-CoA dehydratase PASTICCINO2 is essential and limiting for plant development, *Proc. Natl. Acad. Sci. U. S. A.* 105 (2008), 14727–14731, <https://doi.org/10.1073/pnas.0805089105>.
- [14] F. Beaudoin, K. Gable, O. Sayanova, T. Dunn, J.A. Napier. A *Saccharomyces cerevisiae* gene required for heterologous fatty acid elongase activity encodes a microsomal β -keto-reductase, *J. Biol. Chem.* 277 (2002), 11481–11488, <https://doi.org/10.1074/jbc.M111441200>.

- [15] L. Kunst, L. Samuels. Plant cuticles shine: advances in wax biosynthesis and export, Curr. Opin. Plant Biol. 12 (2009), 721–727, <https://doi.org/10.1016/j.pbi.2009.09.009>.
- [16] T.M. Haslam, L. Kunst. Extending the story of very-long-chain fatty acid elongation, Plant Sci. 210 (2013), 93–107, <https://doi.org/10.1016/j.plantsci.2013.05.008>.
- [17] S. Trenkamp, W. Martin, K. Tietjen. Specific and differential inhibition of very-long-chain fatty acid elongases from Arabidopsis thaliana by different herbicides, Proc. Natl. Acad. Sci. U. S. A. 101 (2004), 11903–11908, <https://doi.org/10.1073/pnas.0404600101>.
- [18] S. Paul, K. Gable, F. Beaudoin, E. Cahoon, J. Jaworski, J.A. Napier, T.M. Dunn. Members of the Arabidopsis FAE1-like 3-Ketoacyl-CoA Synthase Gene Family Substitute for the Elop Proteins of Saccharomyces cerevisiae, J. Biol. Chem. 281 (2006), 9018–9029, <https://doi.org/10.1074/jbc.M507723200>.
- [19] S. Tresch, M. Heilmann, N. Christiansen, R. Looser, K. Grossmann. Inhibition of saturated very-long-chain fatty acid biosynthesis by mefluidide and perfluidone, selective inhibitors of 3-ketoacyl-CoA synthases, Phytochemistry 76 (2012), 162–171, <https://doi.org/10.1016/j.phytochem.2011.12.023>.
- [20] D. Hegebarth, C. Buschhaus, J. Joubès, D. Thoraval, D. Bird, R. Jetter. Arabidopsis ketoacyl-CoA synthase 16 (KCS16) forms C36/C38 acyl precursors for leaf trichome and pavement surface wax, Plant Cell Environ. 40 (2017), 1761–1776, <https://doi.org/10.1111/pce.12981>.
- [21] M. Batsale, M. Alonso, S. Pascal, D. Thoraval, R.P. Haslam, F. Beaudoin, F. Domergue, J. Joubès. Tackling functional redundancy of Arabidopsis fatty acid elongase complexes, Front. Plant Sci. 14 (2023), 1107333, <https://doi.org/10.3389/fpls.2023.1107333>.
- [22] H. Huang, X. Yang, M. Zheng, Z. Chen, Z. Yang, P. Wu, M.A. Jenks, G. Wang, T. Feng, L. Liu, P. Yang, S. Lü, H. Zhao. An ancestral role for 3-KETOACYL-COA SYNTHASE3 as a negative regulator of plant cuticular wax synthesis, Plant Cell 35 (2023), 2251–2270, <https://doi.org/10.1093/plcell/koad051>.
- [23] H. Huang, X. Yang, M. Zheng, S. Lü, H. Zhao. Fine-tuning the activities of β -KETOACYL-COA SYNTHASE 3 (KCS3) and KCS12 in Arabidopsis is essential for maintaining cuticle integrity, J. Exp. Bot. (2023), erad337, <https://doi.org/10.1093/jxb/erad337>.
- [24] A.A. Millar, L. Kunst. Very-long-chain fatty acid biosynthesis is controlled through the expression and specificity of the condensing enzyme, Plant J. 12 (1997), 121–131, <https://doi.org/10.1046/j.1365-3113.1997.12010121.x>.

- [25] M. Ghanevati, J.G. Jaworski. Active-site residues of a plant membrane-bound fatty acid elongase β -ketoacyl-CoA synthase, FAE1 KCS, Biochim. Biophys. Acta 1530 (2001), 77–85, [https://doi.org/10.1016/S1388-1981\(00\)00168-2](https://doi.org/10.1016/S1388-1981(00)00168-2).
- [26] B.J. Blacklock, J.G. Jaworski. Studies into factors contributing to substrate specificity of membrane-bound 3-ketoacyl-CoA synthases, Eur. J. Biochem. 269 (2002), 4789–4798, <https://doi.org/10.1046/j.1432-1033.2002.03176.x>.
- [27] M. Ghanevati, J.G. Jaworski. Engineering and mechanistic studies of the Arabidopsis FAE1 β -ketoacyl-CoA synthase, FAE1 KCS, Eur. J. Biochem. 269 (2002), 3531–3539, <https://doi.org/10.1046/j.1432-1033.2002.03039.x>.
- [28] B. Blacklock, J. Jaworski. Substrate specificity of Arabidopsis 3-ketoacyl-CoA synthases, Biochem. Biophys. Res. Commun. 346 (2006), 583–590, <https://doi.org/10.1016/j.bbrc.2006.05.162>.
- [29] J.Y. Chen, A. Mumtaz, E. Gonzales-Vigil. Evolution and molecular basis of substrate specificity in a 3-ketoacyl-CoA synthase gene cluster from Populus trichocarpa, J. Biol. Chem. (2022), 102496, <https://doi.org/10.1016/j.jbc.2022.102496>.
- [30] P. Böger. Mode of action for chloroacetamides and functionally related compounds, J. Pestic. Sci. 28 (2003), 324–329, <https://doi.org/10.1584/jpestics.28.324>.
- [31] Y. Tanetani, K. Kaku, K. Kawai, T. Fujioka, T. Shimizu. Action mechanism of a novel herbicide, pyroxasulfone, Pesticide Biochem. Physiol. 95 (2009), 47–55, <https://doi.org/10.1016/j.pestbp.2009.06.003>.
- [32] Y. Tanetani, T. Fujioka, K. Kaku, T. Shimizu. Studies on the inhibition of plant very-long-chain fatty acid elongase by a novel herbicide, pyroxasulfone. J. Pestic. Sci. 36 (2011), 221–228. https://www.istage.ist.go.jp/article/jpestics/36/2/36_G10-81/article/-char/en.
- [33] A.J. Jhala, M. Singh, L. Shergill, R. Singh, M. Jugulam, D.E. Riechers, Z.A. Ganie, T.P. Selby, R. Werle, J.K. Norsworthy. Very long chain fatty acid-inhibiting herbicides: Current uses, site of action, herbicide-resistant weeds, and future, Weed Technol. 1–50 (2023), <https://doi.org/10.1017/wet.2023.90>.
- [34] M. Karimi, D. Inzé, A. Depicker. GATEWAY vectors for Agrobacterium-mediated plant transformation, Trends Plant Sci. 7 (2002), 193–195, [https://doi.org/10.1016/s1360-1385\(02\)02251-3](https://doi.org/10.1016/s1360-1385(02)02251-3).
- [35] F. Dittrich-Domergue, J. Joubès, P. Moreau, R. Lessire, S. Stymne, F. Domergue. The bifunctional protein TtFARAT from *Tetrahymena thermophila* catalyzes the formation of both precursors required

- to initiate ether lipid biosynthesis, *J. Biol. Chem.* 289 (2014), 21984–21994, <https://doi.org/10.1074/jbc.M114.579318>.
- [36] R.D. Gietz, R.H. Schiestl, A.R. Willems, R.A. Woods. Studies on the transformation of intact yeast cells by the LiAc/SS-DNA/PEG procedure, *Yeast* 11 (1995), 355–360, <https://doi.org/10.1002/yea.320110408>.
- [37] W. Yang, M. Pollard, Y. Li-Beisson, F. Beisson, M. Feig, J. Ohlrogge. A distinct type of glycerol-3-phosphate acyltransferase with sn-2 preference and phosphatase activity producing 2-monoacylglycerol, *Proc. Natl. Acad. Sci. U. S. A.* 107 (2010), 12040–12045, <https://doi.org/10.1073/pnas.0914149107>.
- [38] J. Liu, Y.-Y. Lee, X. Mao, Y. Li. A simple and reproducible non-radiolabeled in vitro assay for recombinant acyltransferases involved in triacylglycerol biosynthesis, *J. Appl. Phycol.* 29 (2017), 323–333, <https://doi.org/10.1007/s10811-016-0949-6>.
- [39] H.-S. Guo, Y.-M. Zhang, X.-Q. Sun, M.-M. Li, Y.-Y. Hang, J.-Y. Xue. Evolution of the KCS gene family in plants: the history of gene duplication, sub/neofunctionalization and redundancy, *Mol. Genet. Genomics* 291 (2016), 739–752, <https://doi.org/10.1007/s00438-015-1142-3>.
- [40] L. Xu, J. Hao, M. Lv, P. Liu, Q. Ge, S. Zhang, J. Yang, H. Niu, Y. Wang, Y. Xue, X. Lu, J. Tang, J. Zheng, M. Gou. A genome-wide association study identifies genes associated with cuticular wax metabolism in maize, *Plant Physiol.* kiae007 (2024), <https://doi.org/10.1093/plphys/kiae007>.
- [41] C.S. Oh, D.A. Toke, S. Mandala, C.E. Martin. ELO2 and ELO3, homologues of the *Saccharomyces cerevisiae* ELO1 gene, function in fatty acid elongation and are required for sphingolipid formation, *J. Biol. Chem.* 272 (1997), 17376–17384, <https://doi.org/10.1074/jbc.272.28.17376>.
- [42] L. Nie, T. Pascoa, A. Pike, S. Bushell, A. Quigley, G.F. Ruda, A. Chu, V. Cole, D. Speedman, T. Moreira, L. Shrestha, S. Mukhopadhyay, N. Burgess-Brown, J. Love, P. Brennan, E. Carpenter. The structural basis of fatty acid elongation by the ELOVL elongases, *Nat. Struct. Mol. Biol.* 28 (2021), 1–9, <https://doi.org/10.1038/s41594-021-00605-6>.
- [43] P. Böger, B. Matthes, J. Schmalfuß. Towards the primary target of chloroacetamides – new findings pave the way, *Pest Manag. Sci.* 56 (2000), 497–508, [https://doi.org/10.1002/\(SICI\)1526-4998\(200006\)56:6](https://doi.org/10.1002/(SICI)1526-4998(200006)56:6).
- [44] K.E. Stenback, K.S. Flyckt, T. Hoang, A.A. Campbell, B.J. Nikolau. Modifying the yeast very long chain fatty acid biosynthetic machinery by the expression of plant 3-ketoacyl CoA synthase isozymes. *Sci. Rep.* 12 (2022), 13235. <https://doi.org/10.1038/s41598-022-17080-8>.

- [45] T. Götz, P. Böger. The Very-Long-Chain Fatty Acid Synthase Is Inhibited by Chloroacetamides, Z. Naturforsch. C 59 (2004), 549–553, <https://doi.org/10.1515/znc-2004-7-818>.
- [46] J. Schmalfuß, B. Matthes, K. Knuth, P. Böger. Inhibition of Acyl-CoA Elongation by Chloroacetamide Herbicides in Microsomes from Leek Seedlings. Pest. Biochem. Physiol. 67 (2000), 25–35. <https://doi.org/10.1006/pest.2000.2473>.
- [47] C. Lechelt-Kunze, R.C. Meissner, M. Drewes, K. Tietjen. Flufenacet herbicide treatment phenocopies the fiddlehead mutant in Arabidopsis thaliana. Pest. Manag. Sci. 59 (2003), 847–856. <https://doi.org/10.1002/ps.714>.
- [48] T. Furuhashi, M. Otani, M. Iwasa. Dimesulfazet, a novel rice paddy herbicide, is an inhibitor of very long-chain fatty acid biosynthesis. J. Pestic. Sci. 49 (2024), 77–86. <https://doi.org/10.1584/jpestics.D23-036>.
- [49] H. Inui, H. Ohkawa. Herbicide resistance in transgenic plants with mammalian P450 monooxygenase genes. Pest. Manag. Sci. 61 (2005), 286–91. <https://doi.org/10.1002/ps.1012>.
- [50] H. Kawahigashi, S. Hirose, H. Ohkawa, Y. Ohkawa. Transgenic rice plants expressing human p450 genes involved in xenobiotic metabolism for phytoremediation. J. Mol. Microbiol. Biotech. 15 (2008), 212–219. <https://doi.org/10.1159/000121332>.
- [51] Y. Tanetani, K. Kaku, M. Ikeda, T. Shimizu. Action mechanism of a herbicide, thiobencarb. J. Pestic. Sci. 38 (2013), 39–43. <https://doi.org/10.1584/jpestics.D12-047>.
- [52] H. Kawahigashi, S. Hirose, E. Hayashi, H. Ohkawa, Y. Ohkawa. Phytotoxicity and metabolism of ethofumesate in transgenic rice plants expressing the human CYP2B6 gene. Pest. Biochem. Physiol. 74 (2002), 139–147. [https://doi.org/10.1016/S0048-3575\(02\)00153-0](https://doi.org/10.1016/S0048-3575(02)00153-0).

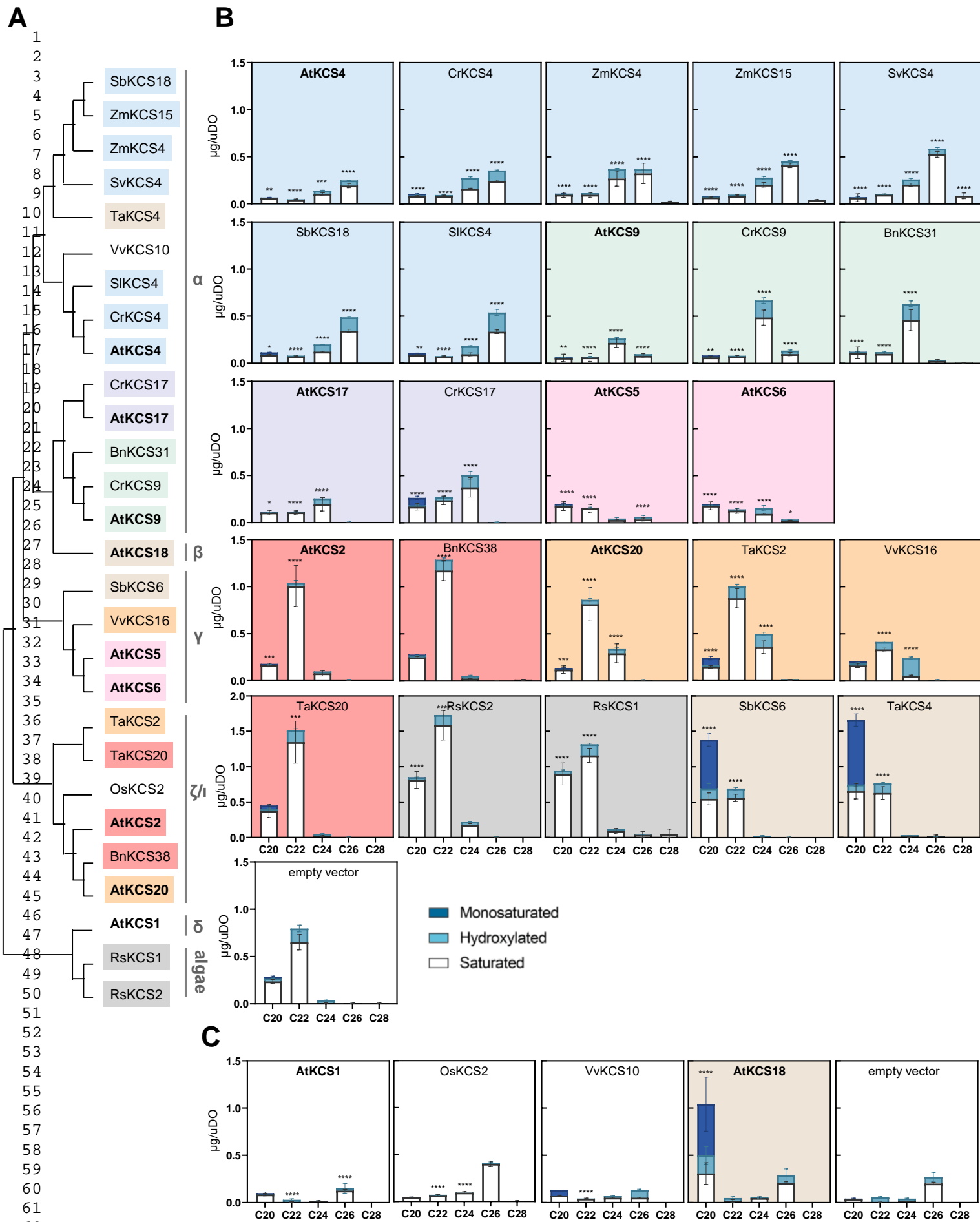
Genes	Species	Accession numbers
<i>AtKCS1</i>	<i>Arabidopsis thaliana</i>	At1g01120
<i>AtKCS2</i>	<i>Arabidopsis thaliana</i>	At1g04220
<i>AtKCS4</i>	<i>Arabidopsis thaliana</i>	At1g19440
<i>AtKCS5</i>	<i>Arabidopsis thaliana</i>	At1g25450
<i>AtKCS6</i>	<i>Arabidopsis thaliana</i>	At1g68530
<i>AtKCS9</i>	<i>Arabidopsis thaliana</i>	At2g16280
<i>ATKCS17</i>	<i>Arabidopsis thaliana</i>	At4g34510
<i>AtKCS18</i>	<i>Arabidopsis thaliana</i>	At4g34520
<i>AtKCS20</i>	<i>Arabidopsis thaliana</i>	At5g43760
<i>BnKCS31</i>	<i>Brassica napus</i>	BnaA07g03590D
<i>BnKCS38</i>	<i>Brassica napus</i>	BnaC05g02350D
<i>CrKCS17</i>	<i>Capsella rubella</i>	CARUB_v10006212
<i>CrKCS4</i>	<i>Capsella rubella</i>	CARUB_v10015226
<i>CrKCS9</i>	<i>Capsella rubella</i>	CARUB_v10011929
<i>OsKCS2</i>	<i>Oryza sativa</i>	BGIOSGA018233
<i>RsKCS1</i>	<i>Raphidocelis subcapitata</i>	GBF96892
<i>RsKCS2</i>	<i>Raphidocelis subcapitata</i>	GBF91682
<i>SbKCS18</i>	<i>Sorghum bicolor</i>	SORBI_3009G236100
<i>SbKCS6</i>	<i>Sorghum bicolor</i>	SORBI_3001G453200
<i>SlKCS4</i>	<i>Solanum lycopersicum</i>	Solyc04g080450
<i>SvKCS4</i>	<i>Setaria veridis</i>	SEVIR_3G144700v2
<i>TaKCS2</i>	<i>Triticum aestivum</i>	TraesCS6B02G207000
<i>TaKCS20</i>	<i>Triticum aestivum</i>	TraesCS7B02G254900
<i>TaKCS4</i>	<i>Triticum aestivum</i>	TraesCS1B02G436300
<i>VvKCS10</i>	<i>Vitis vinifera</i>	Vitvi18g00969
<i>VvKCS16</i>	<i>Vitis vinifera</i>	Vitvi14g01198
<i>ZmKCS15</i>	<i>Zea mays</i>	GRMZM2G160417
<i>ZmKCS4</i>	<i>Zea mays</i>	GRMZM2G393897

Table S1. Accession number list of the 28 KCS genes expressed in yeast.

Q1 [M+H] ⁺	Q3 [M+H] ⁺	ID	Dwell time (ms)	Cone (V)	CE (V) collision energy
1035	528	CoA18:0	10	5	45
1049	542	CoA18:0-oxo	10	5	45
1063	556	CoA20:0	10	5	45
1077	570	CoA20:0-oxo	10	5	45
1091	584	CoA22:0	10	5	45
1105	598	CoA22:0-oxo	10	5	45
1119	612	CoA24:0	10	5	45
1133	626	CoA24:0-oxo	10	5	45
1148	641	CoA26:0	10	5	45
1161	654	CoA26:0-oxo	10	5	45

Table S2. MS/MS transitions in HPLC-UV-MS/MS.





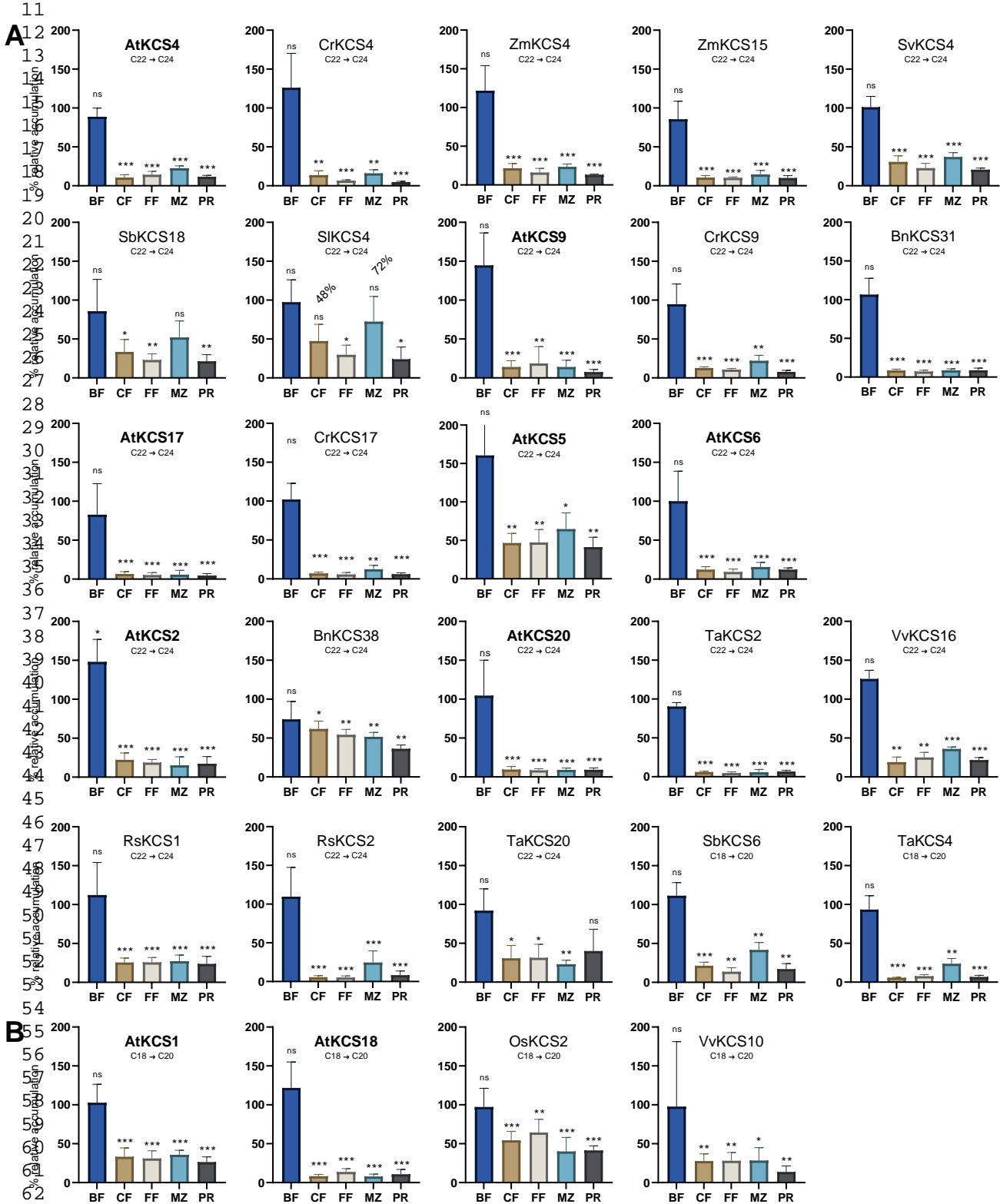


Figure 3

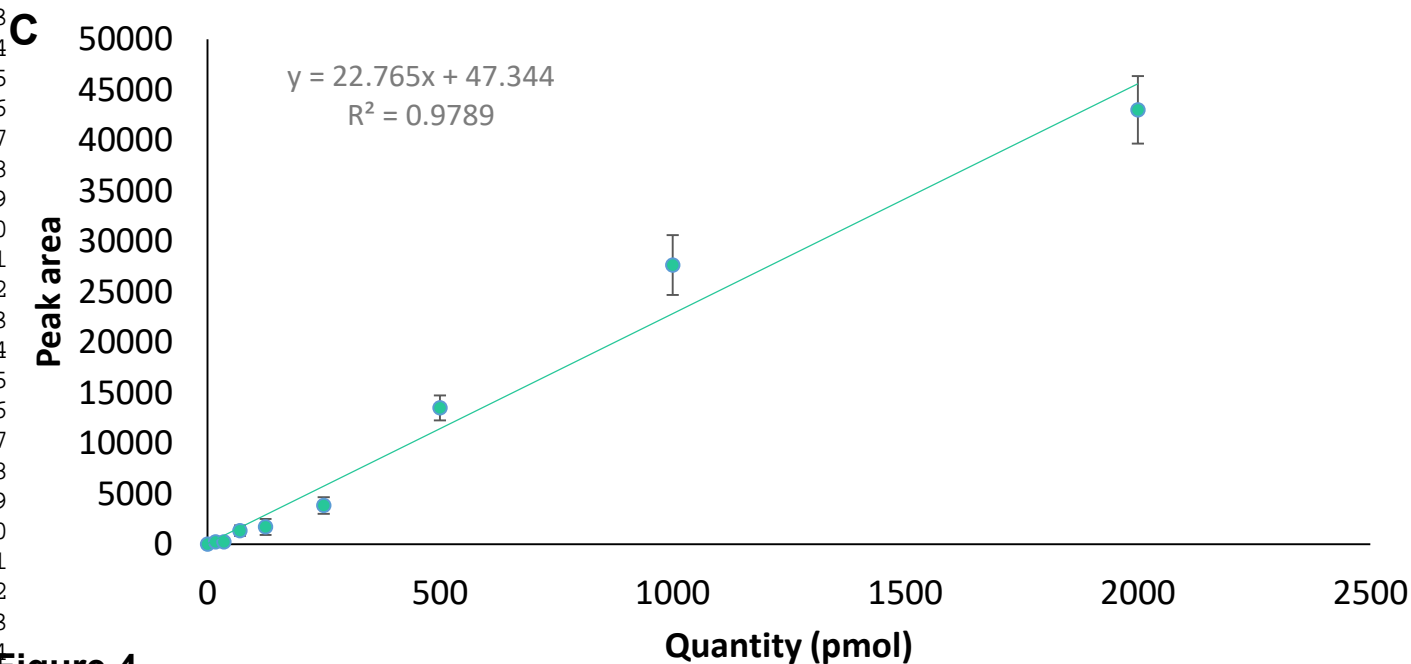
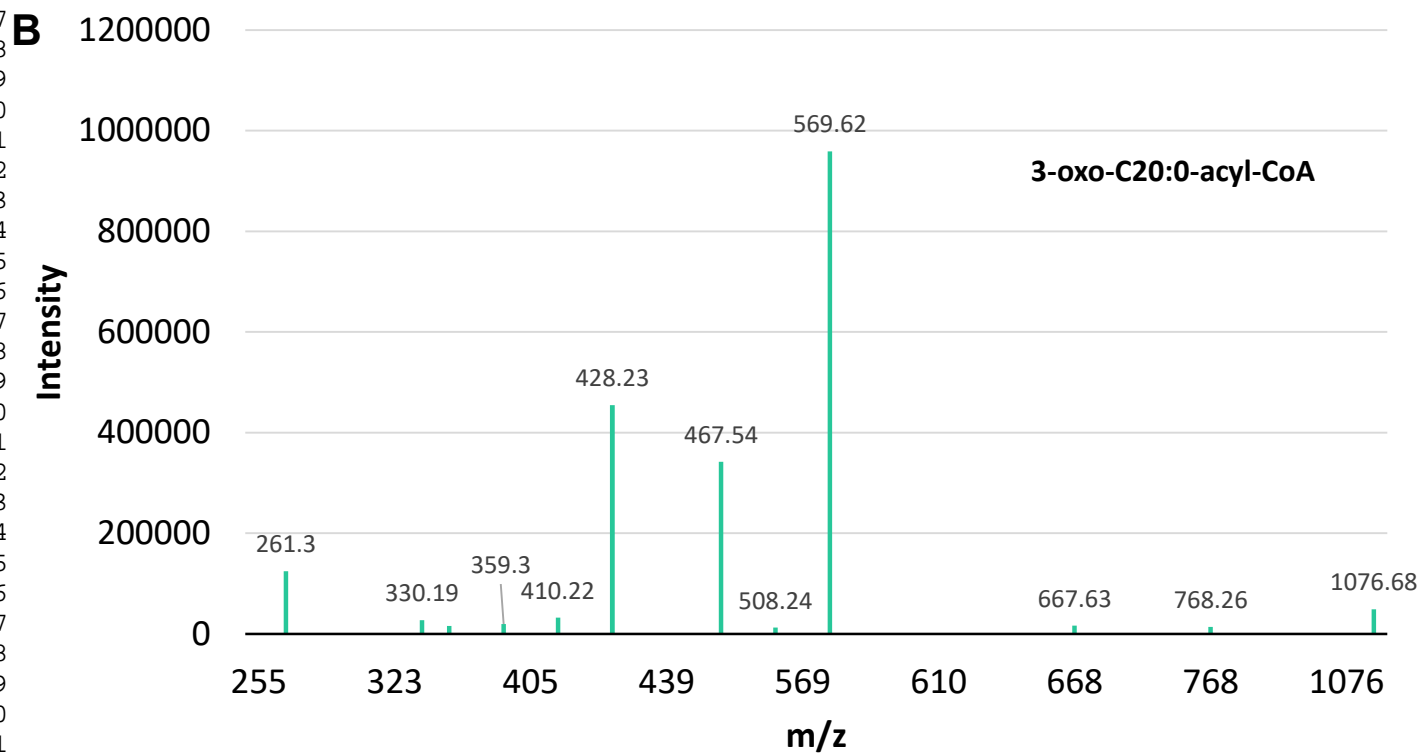
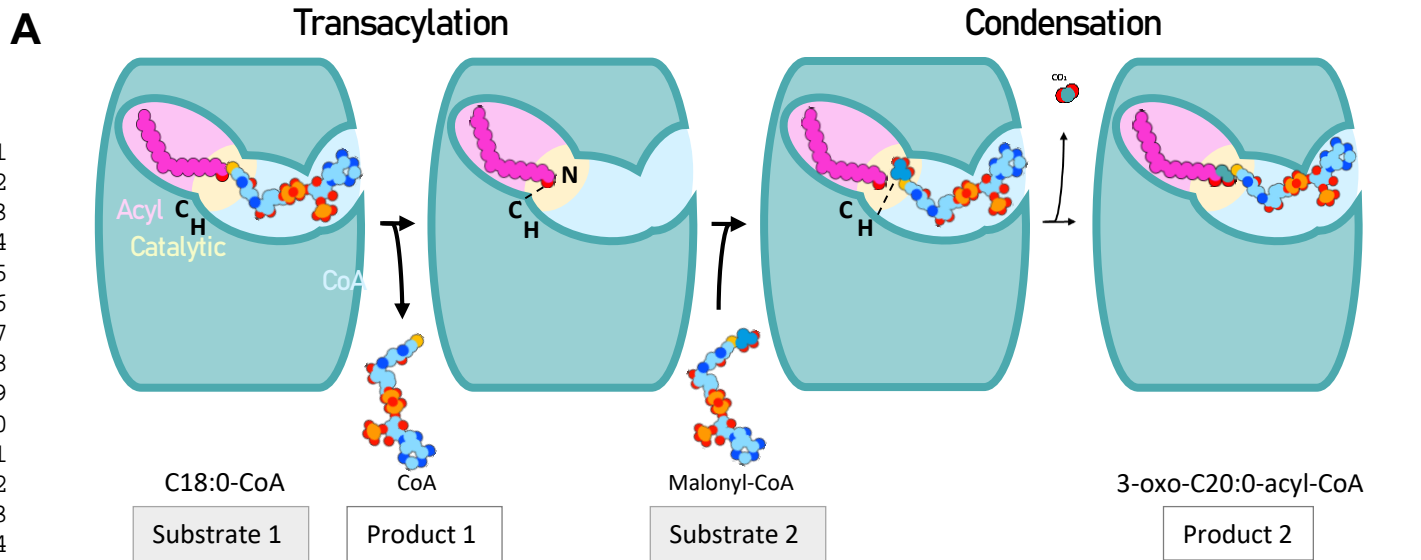
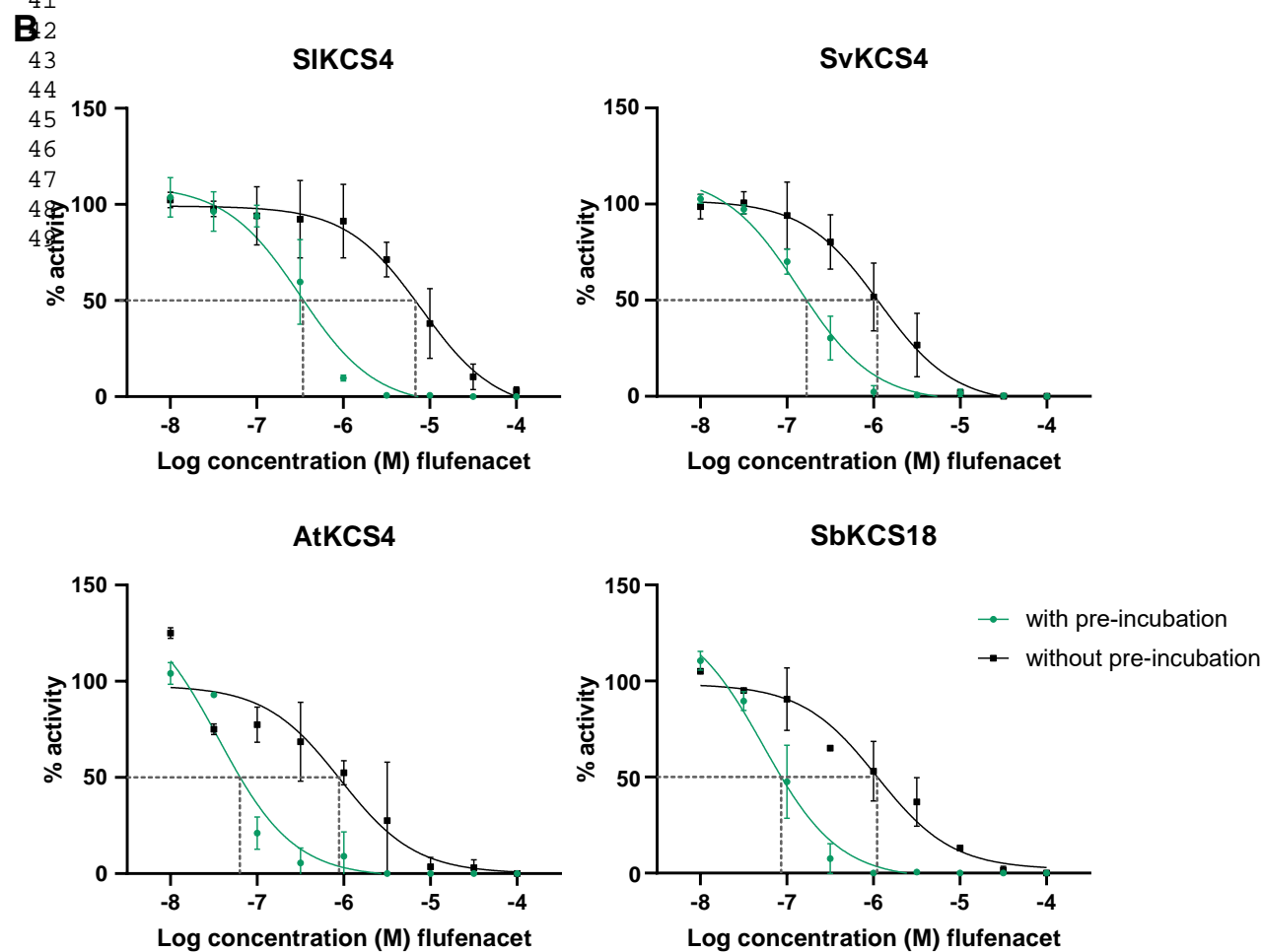
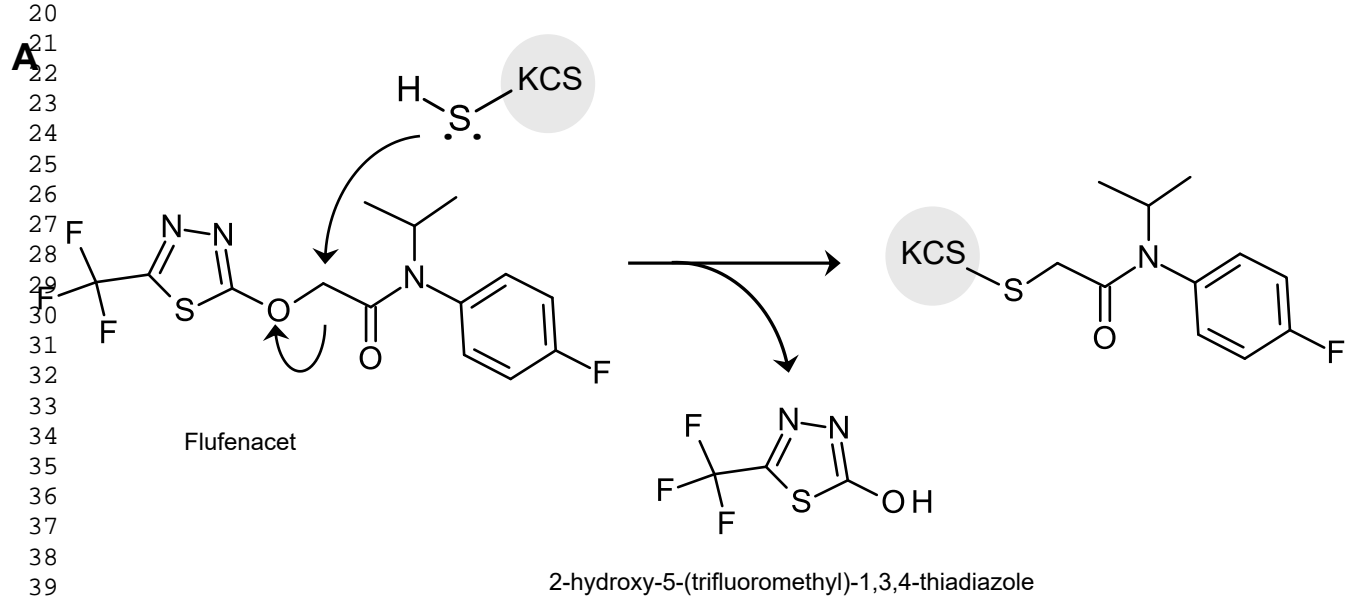


Figure 4



C

IC ₅₀ [M]	With pre-incubation	Without pre-incubation
SIKCS4	3.2 · 10 ⁻⁷	79.8 · 10 ⁻⁷
SvKCS4	1.4 · 10 ⁻⁷	11.5 · 10 ⁻⁷
AtKCS4	0.4 · 10 ⁻⁷	9.12 · 10 ⁻⁷
SbKCS18	0.5 · 10 ⁻⁷	11.0 · 10 ⁻⁷

Figure 5

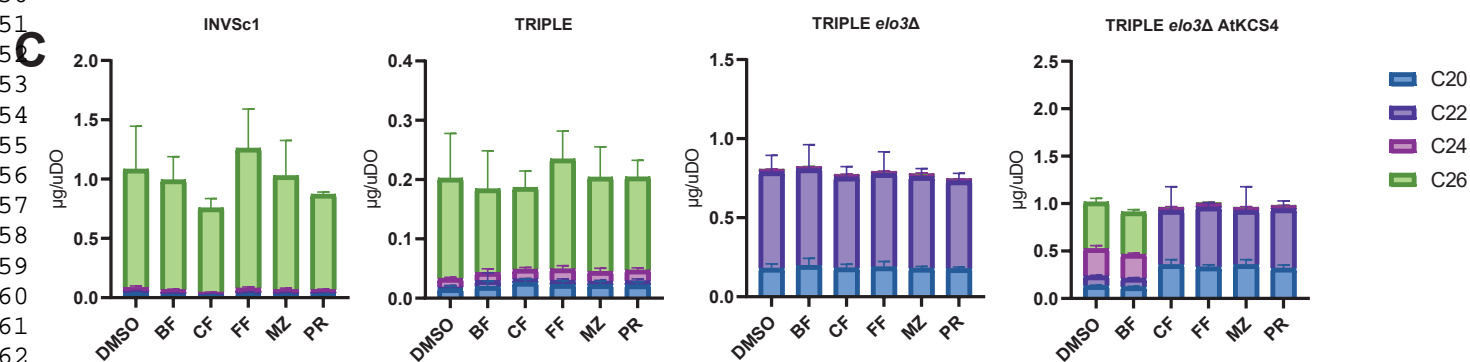
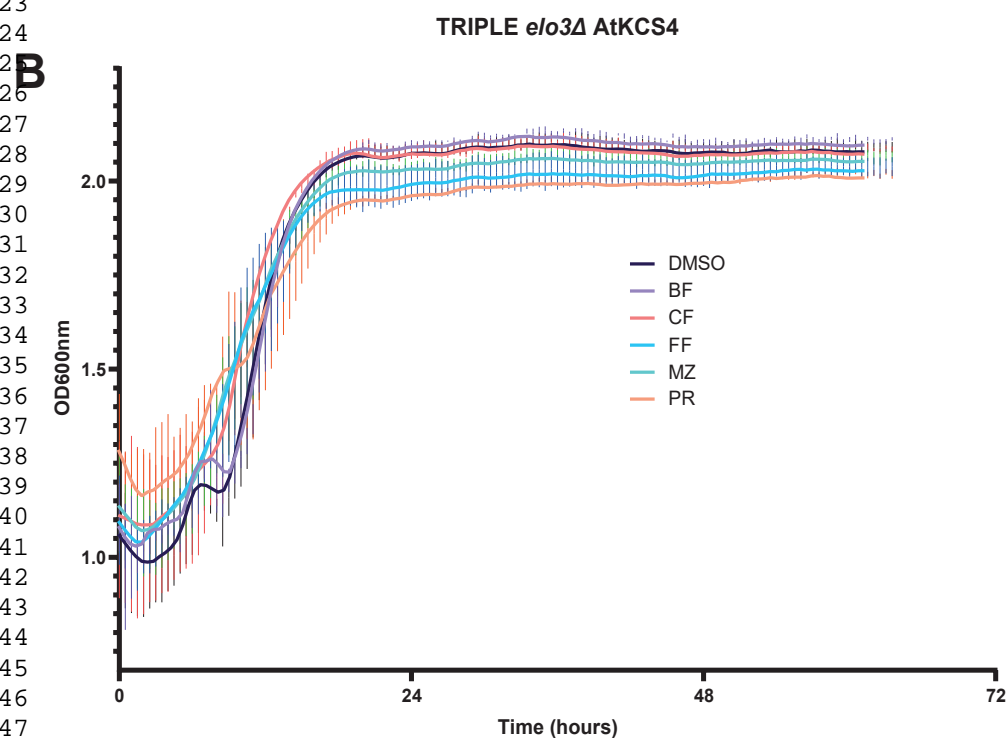
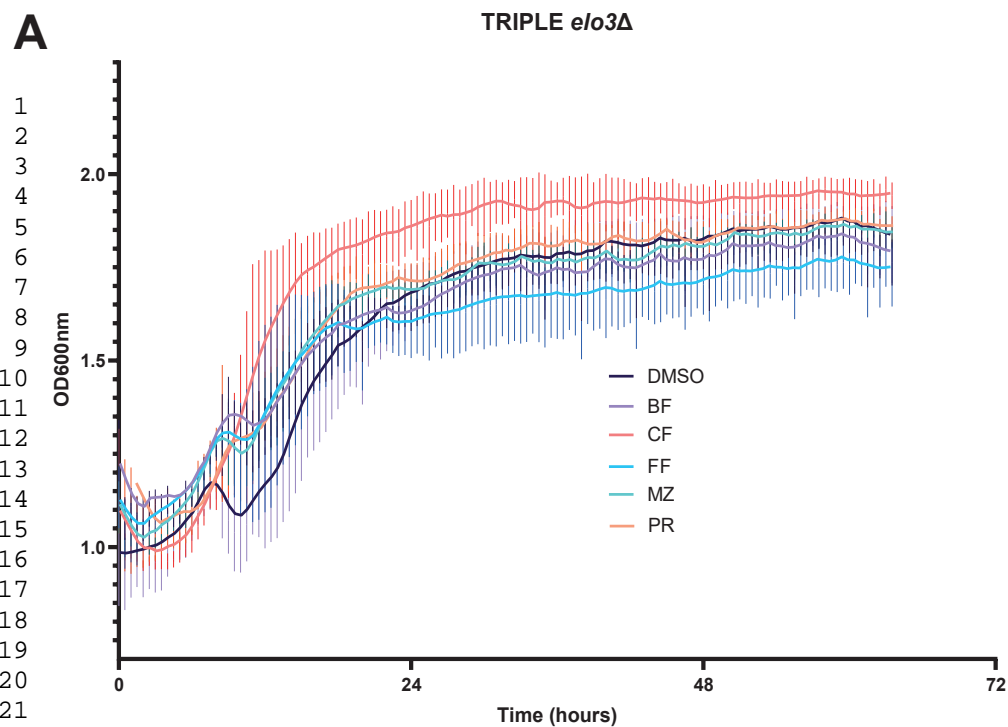


Figure S1

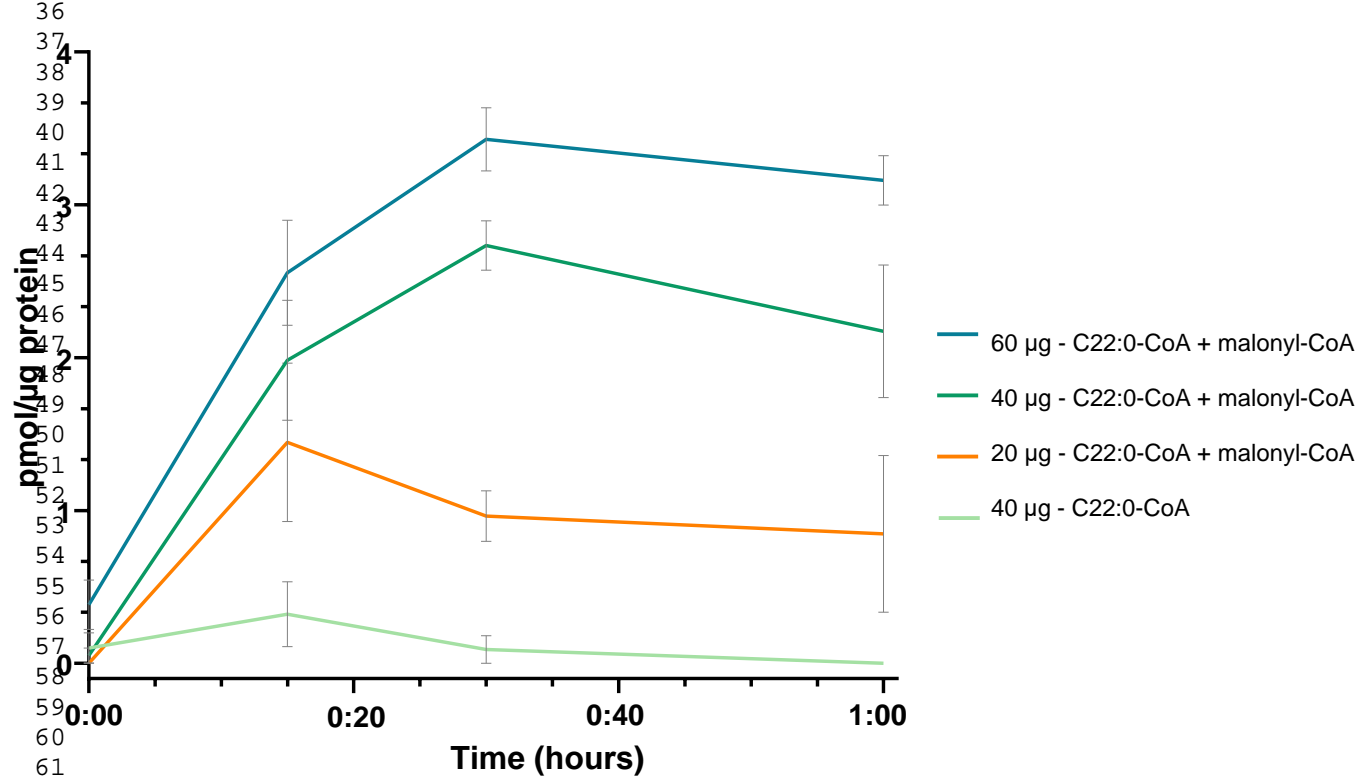


Figure S2